

What Matters in Building Vision-Language-Action Models for Generalist Robots

Xinghang Li^{1,2,6}, Peiyan Li^{2,3}, Long Qian⁶, Minghuan Liu^{2,4}, Dong Wang^{1,2}, Jirong Liu^{2,4}, Bingyi Kang², Xiao Ma², Xinlong Wang⁶, Di Guo⁷, Tao Kong^{2,✉}, Hanbo Zhang^{5,✉}, Huaping Liu^{1,✉}

¹Department of Computer Science and Technology, Tsinghua University,

²ByteDance Research, ³CASIA MAIS-NLPR,

⁴Shanghai Jiao Tong University, ⁵National University of Singapore

⁶Beijing Academy of Artificial Intelligence, ⁷Beijing University of Posts and Telecommunications

taokongcn@gmail.com, zhanghb@comp.nus.edu.sg,

hpliu@tsinghua.edu.cn

Abstract

To utilize Foundation Vision Language Models (VLMs) for robotic tasks and motion planning, the community has proposed different methods for injecting action components into VLMs and building the Vision-Language-Action models (VLAs). In this work, we disclose the key factors that significantly influence the performance of VLA on robot manipulation problems and focus on answering three essential design choices: which backbone to select, how to formulate the VLA architectures, and when to add cross-embodiment data. The obtained results convince us firmly to explain why we prefer VLA and develop a new family of VLAs, RoboVLMs, which require very few manual designs and achieve a new state-of-the-art performance in three simulation tasks and real-world experiments. Through our extensive experiments, which include over 8 VLM backbones, 4 policy architectures, and over 600 distinct designed experiments, we provide a detailed guidebook for the future design of VLAs. In addition to the study, the highly flexible RoboVLMs framework, which supports easy integrations of new VLMs and free combinations of various design choices, is made public to facilitate future research. We open-source all details, including codes, models, datasets, and toolkits, along with detailed training and evaluation recipes at: [robovlms.github.io](https://github.com/robovlms).

Index Terms

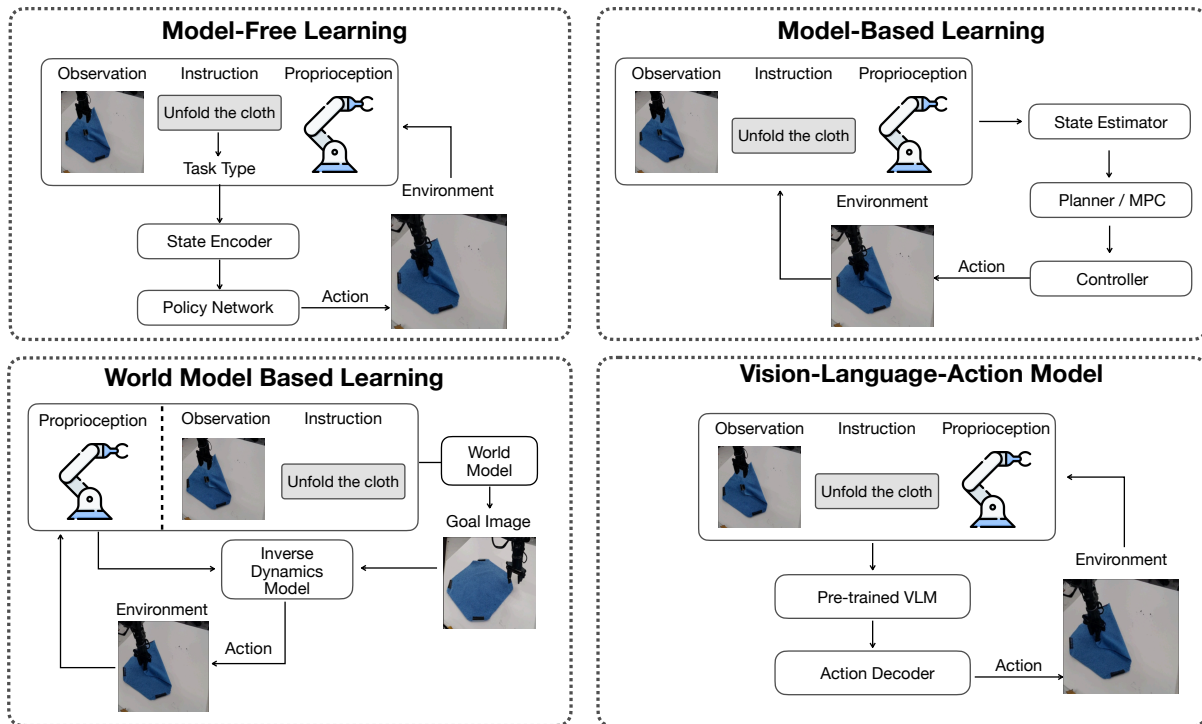
Robot Foundation Models, Vision-Language-Action Models, Generalist Robot Policies

I. INTRODUCTION

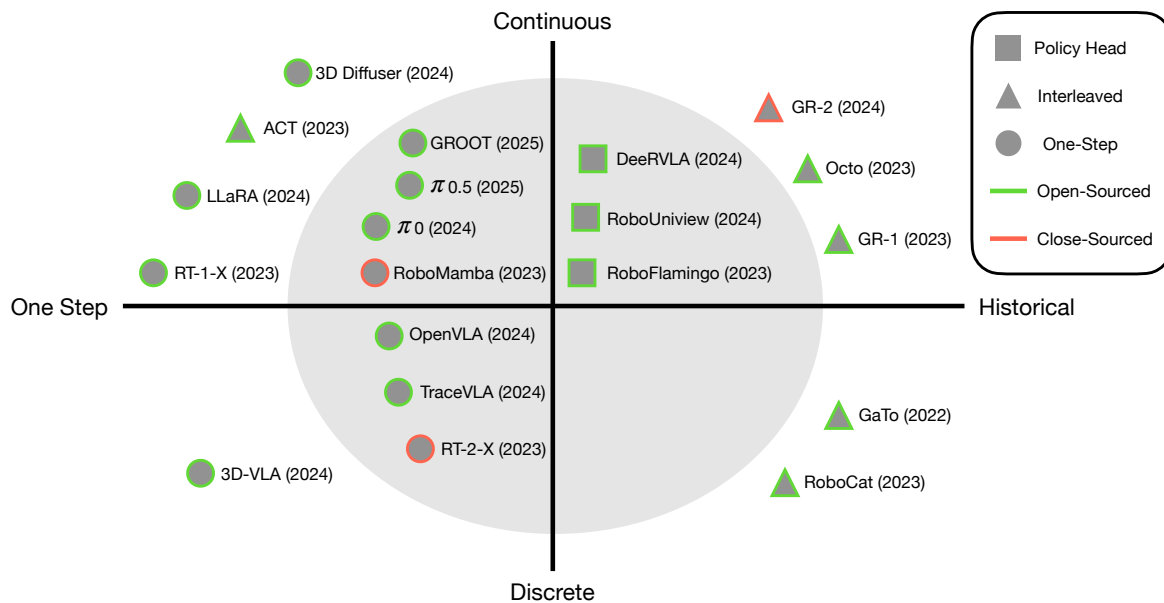
Building generalizable robot policies capable of perceiving, reasoning, and interacting with the physical environment given human instructions has been a long-standing challenge in robotics [4, 5, 7, 27, 33]. Recently, there has been an active exploration of *Vision-Language-Action Models* (VLAs), namely, a family of learning-based robot foundation models directly built upon generalist *Vision-Language Models* (VLMs), and they have demonstrated promising results of semantic generality in both simulated and real-world tasks [7, 20, 22] (Although the rigorous definition of VLAs is not consistent in different works, we regard the ones directly built upon large-scale VLMs along with robot-domain data as the key factor to identify VLAs in this work.). As shown in Fig. 1a, existing robot policies can be categorized into four main groups: (1) **Model-Free Learning**, which encode the state into a latent representation and use a policy network to predict actions, enabling generalization across different embodiments; (2) **Model-Based Learning**, which rely on the robot’s affordances and explicit models of the robot and environment, limiting their applicability to specific configurations; (3) **World Model Based Learning**, which predicts future goal images and derives actions via inverse dynamics models; and (4) **Vision-Language-Action (VLA) Model**, representing a specialized branch of model-free learning that leverages the generalization and robustness of Vision-Language Models (VLMs) by employing them as state encoders. Therefore, a natural question arises: **Why** do we prefer VLAs built upon large-scale pre-trained VLMs? As shown in Fig. 1a, VLA is a newly raised model-free learning framework that receives natural language instruction as input and learns a generalist policy, rather than task-specific policies in traditional model-free learning. The widely-believed reason is that VLAs may inherit the power of VLMs, which have been shown powerful in learning generalized and robust representations of multi-modal data, such as text, images/videos, through extensive training on web-scale data. Such capabilities can facilitate the adaptation of robot foundation models to highly diverse open-world scenes with limited robotic data. However, it remains an open problem how large-scale vision-language pre-training facilitates generalist robot policies.

While VLAs have shown early promise, effectively transferring pre-trained VLMs into high-performing robot policies remains non-trivial. Challenges still remain in how to sufficiently and efficiently select and utilize: 1) vision-language backbones; 2) formulation that best leverages multi-modal representations; and 3) the increasing robot data. As shown in Fig. 2, to address these challenges, we focus on three critical questions:

1. Which kind of VLM backbones are suitable for VLAs? Selecting an appropriate VLM backbone is a fundamental yet underexplored design choice in adapting vision-language models for robotic control. Modern VLMs vary widely in architecture. They differ in model capacity, visual encoder structure, fusion mechanisms, and data scale. While these models are originally



(a) The illustration of strategies of learning-based robot policies. The existing robot policies can be categorized into the following four classes: Model-Free Learning, Model-Based Learning, World Model Based Learning, and Vision-Language-Action Model. The former three formulations consider the language-conditioned manipulation in different manners: Model-free Learning encodes the state into latent variables and utilizes a task-specific policy network to predict the action. Model-based learning solves the manipulation problem by decomposition. Yet, for tasks with complex dynamics (e.g., opening doors or cutting apples), an accurate dynamics model is demanded, while it is extremely hard to learn and generalize. World-model-based learning predicts the goal states (e.g., the goal image) and predicts actions accordingly. While the vision-language-action model is a specific branch of model-free learning, which fully exploits the generalization and robustness of vision-language models (VLMs), and utilizes VLMs as the state encoder, facilitating strong performance on unknown object semantics and instruction following.



(b) The structure categorization of the existing generalist policies and recent works, based on two primary levels: 1) action space (vertical axis); and 2) whether the history information is integrated (horizontal axis). Moreover, for the VLAs that involved history, we split the VLAs that involved history into policy head and interleaved formulation based on the organization pattern of the history information. Note that this categorization not only considers models derived from pre-trained VLMs but also encompasses policy architectures that, while not pre-trained on VLMs (and therefore not claimed as VLAs), can provide insights into transforming VLMs into VLAs. Note that the works lied in the gray circle refer to the VLMs-based VLAs.

Fig. 1: The strategies of learning-based robot policies and the categorization and the recent generalist policies.

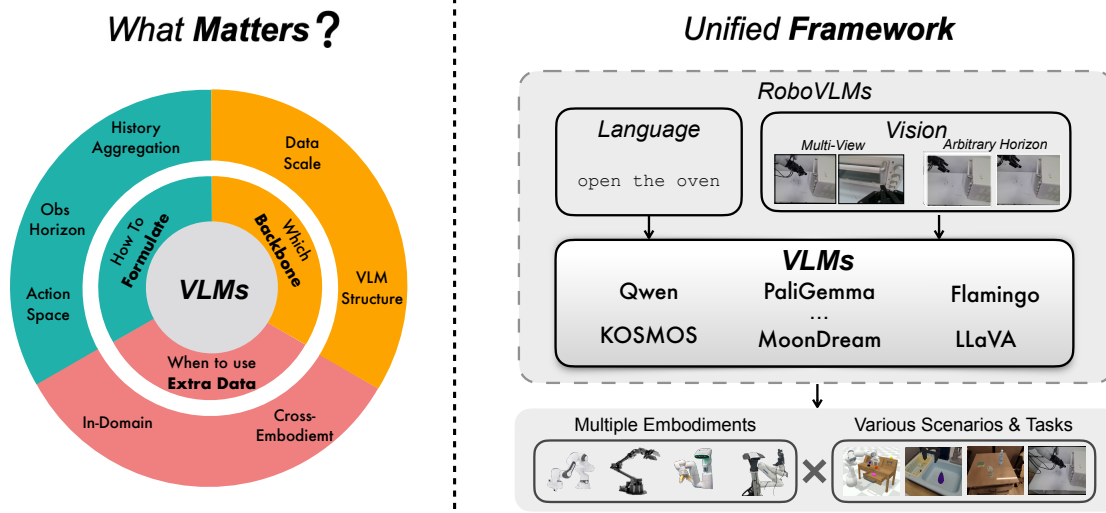


Fig. 2: This work mainly considers three key ingredients for building VLAs based on VLMs: **How** to formulate the problem modeled by VLAs (*i.e.*, observation horizon, action space, and how to aggregate history knowledge); **Which** backbone to use (*i.e.*, various VLM structures, and the data scaled used for the VLM training); and **When** to use extra data source to improve the VLA performance in the tested scenario (*e.g.*, in domain robot data on different tasks, and cross-embodiment data). With our proposed *RoboVLMs*, we can easily transfer various VLMs into generalist robot policies, while supporting multiple embodiments, scenarios, and tasks.

trained for general vision-language tasks, their effectiveness in policy learning depends on how well they can encode physical object properties, spatial relationships, and task-relevant semantics. Existing works are based on diversified VLM structures, and most of them show promising results on adaptation to diverse and complicated manipulation skills. Yet, there is no comprehensive study on how backbone choices impact downstream robot manipulation performance, and hence, it remains an open problem: Which kind of VLM backbones facilitates the VLA learning most.

2. How should VLAs be formulated to best leverage VLMs? Beyond the diversity of different backbones, for generalist robot policies, including VLAs, the structures are more complex and vary in form. Based on the most prevalent existing work [4, 7, 18, 20, 22, 32, 33, 38, 45, 53], we propose a categorization based on 1) how the history and action information are incorporated in VLAs and 2) whether the action space is continuous or discrete. As shown in Fig. 1b, four types of structure formulations are considered. For history information modeling, two forms are identified: 1) one-step modeling, which utilizes only the current state or observation to produce actions; and 2) history modeling, which processes a sliding window of historical states or observations. Regarding the aggregation of history information, we classify it into two approaches: a) interleaved modeling, which integrates historical observation and action sequences in an interleaved format; and b) policy head, which separately processes each historical step and fuses the information at a distinct policy head for action prediction. These above-mentioned formulations leverage the pre-trained VLMs in their different ways. Hence, they may have different features in terms of robustness, generalization ability, and data efficiency when faced with various types of environments and tasks. Therefore, it is practically important but underexplored to understand: How should we formulate VLAs to sufficiently leverage the power of VLMs in practice?

3. When should we leverage the public diverse robot data for optimal training? In addition to the VLA itself, the quality and diversity of the training data used to develop VLAs are equally critical. With recent progress achieved by well-known VLAs [4, 7, 20, 33, 38], large-scale data from different embodiments (also known as cross-embodiment data) is important to further improve performance in terms of robustness and generalization against out-of-distribution tasks and environments. Yet, they differ largely in detailed training recipes: some utilize cross-embodiment data to 1) pre-train a foundation VLA from VLMs by refining representations closer to robotic manipulation tasks [4, 54] and 2) post-train the VLA with in-domain data; while others co-train VLAs with cross-embodiment data alongside in-domain data [7, 20, 33, 38]. Moreover, by being sufficiently pre-trained on cross-embodiment datasets, VLAs are expected to learn new skills with minimal demonstrations [12]. Consequently, in the case of developing efficient VLAs, when to leverage the large-scale cross-embodiment data becomes an intriguing issue.

To thoroughly study the aforementioned key questions, we propose a general framework, **RoboVLMs**, to easily transfer the VLMs into VLAs and implement a fair comparison. We evaluate these models on two popular robot manipulation benchmarks in simulation: **CALVIN** [30] and **SimplerEnv** [35]. Moreover, we also trained and evaluated the built VLAs on a real-world robot manipulation dataset, consisting of 100 manipulation tasks and a total of 74K trajectories. Specifically, we initially selected

three commonly used VLMs—LLaVA, Flamingo, and KosMos, as backbones, combining each with the four VLA structures illustrated in Fig. 1b to examine the effects of action space, observation horizon, and history aggregating methods. With the finding that the policy head modeling with continuous action space performs best, we compare 8 various VLMs as the backbone with policy head formulation to answer which backbone is more suitable. Meanwhile, we compare the generalization and data efficiency of different VLA structures. For the question of when to leverage cross-embodiment data, we compare co-training (the VLAs trained with Open X-Embodiment), finetuning (the VLAs trained with the target dataset), and post-training (the VLAs co-trained with Open X-Embodiment and further finetuned with the target dataset). Finally, to confirm the real-world applicability of the VLAs with the optimal configuration, we trained and evaluated them in real-world robot manipulation scenarios, demonstrating generalization across 1) unseen distractors, 2) unseen backgrounds, 3) unseen target objects, and 4) novel skill descriptions.

Through our extensive and comprehensive studies, we derive conclusions on how to build high-performance VLAs around the following questions:

Why do we prefer VLAs? VLAs built upon pre-trained VLMs have proven to be both effective and efficient for generalist robot policies. Across all experiments, including simulations and real-world manipulation tasks, our VLA consistently outperforms open-source state-of-the-art VLAs by a significant margin. Furthermore, pre-trained VLMs exhibit notable advantages in generalization and data efficiency, making them highly desirable for real-world robotic applications.

Which VLM backbone is more suitable for VLAs? Our extensive study on 8 different VLM backbones shows two distinguished VLM backbones, namely KosMos [34] and Paligemma [3], which significantly outperform the others. These results highlight that comprehensive vision-language pretraining is essential for achieving superior VLA performance.

How should we formulate VLAs? Through extensive study and experiments, continuous actions consistently outperform auto-regressive discrete actions, while incorporating historical context is crucial for enhancing performance and addressing partial observability. For the model architecture, Vision-Language Models (VLMs) integrated directly with policy heads demonstrate superior performance compared to other formulations due to the consistent usage, i.e., vision-language tokens should be processed in their original pretraining format, with a policy head added to integrate past visual and proprioceptive observations for effective decision-making. Finally, larger VLMs further enhance efficiency, requiring fewer data to achieve higher performance.

When should we leverage cross-embodiment datasets? While it is widely believed that pre-training or post-training with cross-embodiment data improves performance, this belief has not been rigorously validated. Our findings reveal that pre-training with cross-embodiment data does not consistently yield significant improvements in final performance. However, post-training a cross-embodiment pre-trained model on the target dataset can lead to notable performance gains. Additionally, leveraging manipulation data from the same robots or tasks provides a clear boost in performance.

II. MAIN RESULTS AND FINDINGS

The primary objective of this work is to establish VLAs as robust generalist robotic policies by thoroughly analyzing contemporary VLA architectures and identifying the key factors driving their performance.

As shown in Extended Table. 1, we aim to answer the four questions (why/which/how/when) described in the former section. The 4 questions are further divided into 6 executable research problems, and successively experiments are designed to answer each.

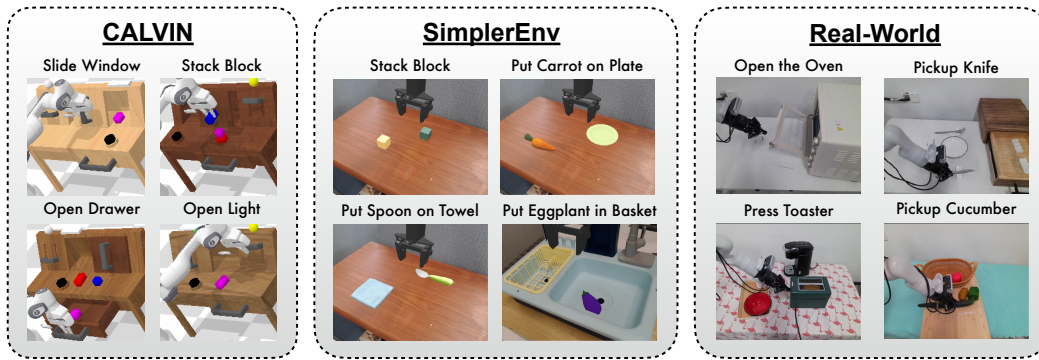
A. Benchmarks and Evaluation Metrics

To comprehensively evaluate the performance of VLAs, in this work, we benchmark all models on a diverse set of benchmarks and robotic manipulation tasks in both simulation and the real world. Specifically, as shown in Fig. 3a, we choose two well-known and widely-used simulation benchmarks (**CALVIN** [30] and **SimplerEnv** [39]) as our testbed. Moreover, we deploy and test our system on a real-world robot manipulation benchmark, including more than 100 tasks, to evaluate RoboVLMs.

CALVIN [30] is a simulation benchmark for multitask table-top manipulation. The dataset contains four splits A, B, C, and D according to different scene settings and provides 34 basic tasks with 24K human teleoperated demonstrations annotated with language instructions in total. Evaluation metrics include the success rates of finishing 1 ~ 5 consecutive tasks, as well as the average number of achieved tasks successfully executed (shortened as *Avg. Len.*).

SimplerEnv [23] is designed as a suite of real-to-sim environments and enables the evaluation of robot policies in simulation. It creates a comparable arena for benchmarking the success rate of robot policies in private real-world settings such as Google Robot [6, 7] and Bridge V2 [43]. Evaluation metrics for **SimplerEnv** are the success rate of each task, simply counted by the number of successfully finished tasks over all valid trials.

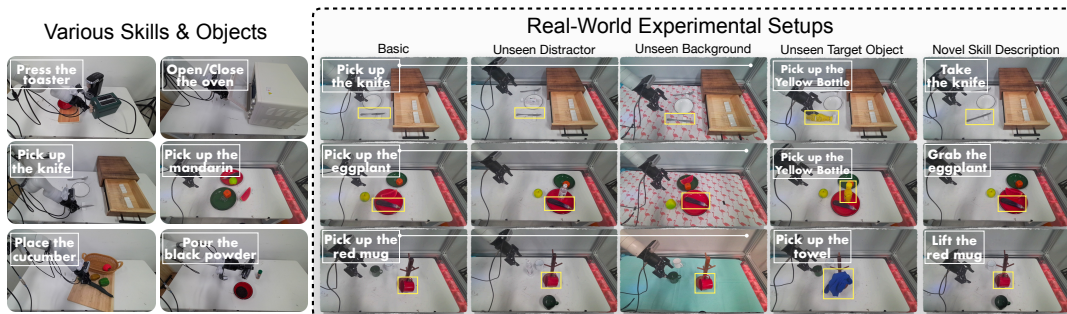
Real Robot Benchmark [8] consists of over 70K teleoperated human trajectories used to fine-tune robot policies, covering 105 manipulation tasks. To evaluate the performance of models on this benchmark, we adopt the approach outlined in [21], testing each model on one *Simple* setting and four challenging *Unseen* settings. Examples of these settings are shown in Fig. 3c. In total, we evaluate each VLA across 20 tasks, with 5 settings per task and 3 rollouts per setting, reporting the average success rate for each setting. A detailed description of the benchmarks is provided in Appendix.



(a) Two simulated and one real-world benchmarks. We show environment setups and example tasks involved.



(b) The demonstration of our real robot platform. The platform is equipped with a side camera and a wrist camera.



(c) The illustration of the experimental settings in real-world experiments. We evaluate the models in 20 tasks with five settings for each task, involving Unseen Distractor, Unseen Target Object and Unseen Background, Novel Skill Description

Fig. 3: Illustration of the involved simulations and real-world benchmarks.

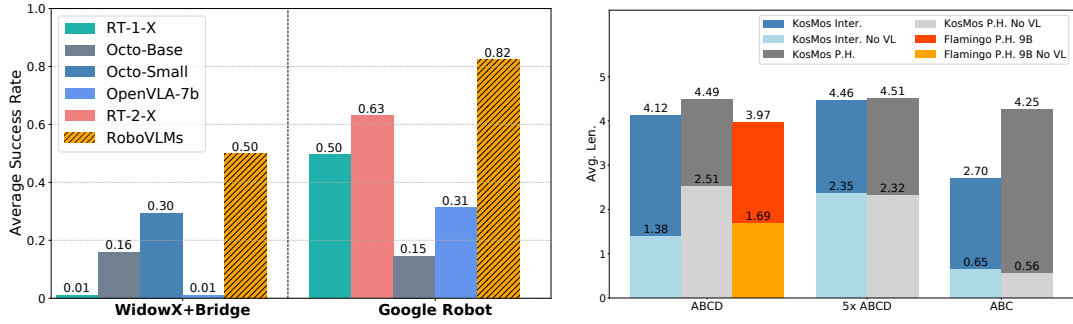
B. Why do we prefer VLAs?

This section investigates one of the key questions: *Why do we want VLAs?* To answer this question, we need to answer the following prerequisite sub-question first:

Question 1.1: Are VLAs a proper choice for building generalist robot policies?

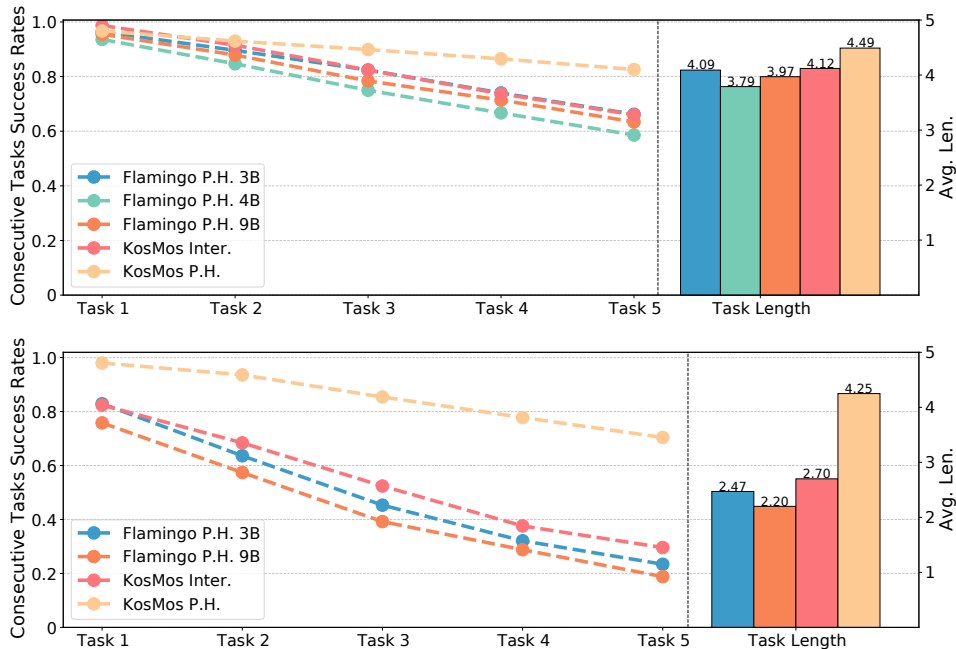
Concretely, we demonstrate the best-performing VLA resulting from our study, which sets a new state-of-the-art result on both **CALVIN** and **SimplerEnv** benchmarks, outperforming all other robot policies with a clear margin. All results are shown in Extended Table. 2 and Fig. 4a. From these tables, we can see that our strongest RoboVLM exceeds the existing state-of-the-art generalist policies by a large margin and establishes a strong baseline for robot manipulation tasks both in simulation and real-world experiments. Concretely, we can easily observe the following facts:

- On **CALVIN** benchmark, our best model achieves the highest performance in all metrics and demonstrates superior generalization ability when transferring from ABC to D (a novel scene unseen in the training splits) with an absolute improvement of 12.6% for the execution of a single task and a total improvement of 30.3% for 5 consecutive tasks. On

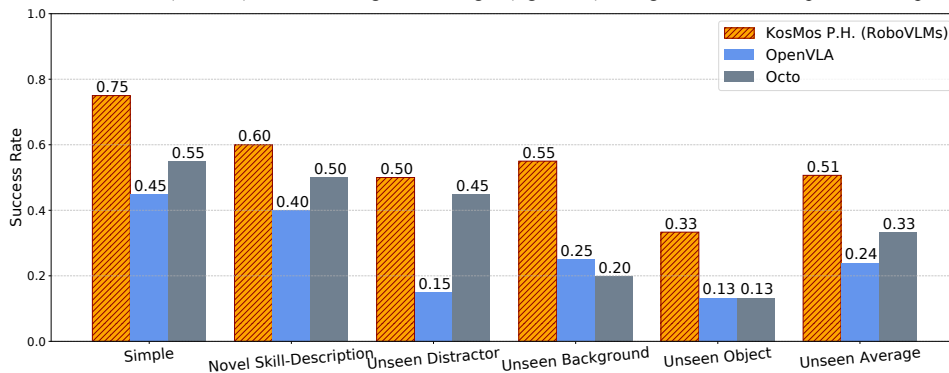


(a) Evaluation results on the SimplerEnv simulation benchmarks, including the WidovX+Bridge and Google Robot environments. Performance of baseline methods are referred from Li et al. [23]. The KosMos P.H. built by RoboVLMs is the best VLA structure investigated, which is trained over fixed training steps. Detailed numerical results can be further referred to Extended Table. 3.

(b) Ablation study of VLAs for vision-language pre-training on different settings of the CALVIN benchmark. “P.H.” denotes policy head. “No VL” suggests models without VL pre-training. “Inter” refers to the interleaved formulation. “5x” represents training with 5x re-generated training data. Full results on different training settings and data scales are shown in Appendix.



(c) Performance on CALVIN benchmark, all models are trained on split ABC/ABCD, and evaluated on split D (the upper figure is trained on ABC, and the lower figure ABCD). We report the success rates of five consecutive tasks (left axis) and the averaged task length (right axis), using the model checkpoint at 5th epoch.



(d) Real-robot performance of our best VLA (KosMos P.H.) built by RoboVLMs against baseline methods over different settings. RoboVLM outperforms the existing VLAs over all settings, especially for metrics in unseen scenarios, demonstrating the effectiveness and robustness of our model.

Fig. 4: The experimental results for RoboVLMs in Simulations and real world.

average, under zero-shot settings, our model can finish 4.25 tasks out of 5 tasks for each single rollout, outperforming the previous SOTA model (GR-1) by 1.19 tasks.

- On **SimplerEnv**, our model achieves the highest average performance on both *WidowX + Bridge* and *Google Robot* environments, demonstrating the general effectiveness and robustness against different settings and diverse manipulation tasks.

We also investigated the impact of vision-language pre-training on the generalization and data efficiency (Fig. 4b and Extended Table. 4). For the generalization in CALVIN, we adopt the official setting: training models on the split of ABC and validating performance on D. To evaluate data efficiency, we conduct experiments on model scales ranging from 3B to 9B and various data scales: 10% training data (**0.1x ABCD**), the standard setting (**ABCD**), and 500% training data (**5x ABCD**). The additional data originates from the officially released unlabeled datasets, following the setups as introduced in Wu et al. [45]. The detailed results on different data scales are shown in Appendix.

We can see that vision-language pre-training is essential for both generalization and data efficiency. This observation is intuitive, as an aligned vision-language representation provides a robust foundation for visual understanding, enabling the policy to focus on learning manipulation skills. Therefore, we can conclude that

Finding 1.1: VLA is a promising path to generalist robot policies.

However, although VLAs perform well in simulation, it is still an open problem whether VLAs are suitable for real-robot applications due to the sim-to-real gap [52]. We propose the second open question:

Question 1.2: How does the best VLA built with RoboVLMs perform in real-world scenarios?

As discussed above, we deploy the best-performing RoboVLM model, that is, the one based on the decoder-only KosMos in real-world scenarios to validate its effectiveness. As shown in Fig. 3c, our experiment involves 20 tasks with multiple skills, including *Open*, *Close*, *Press Button*, *Pick & Place*, etc. For each task, we evaluate five settings, with the basic setting, novel skill description, unseen distractors, unseen target object, and unseen background.

Our robot system for real experiments is built on a 7-DoF Kinova Gen3 robot arm paired with a Robotiq 2F-85 gripper. Please refer to Sec. III for more details of the real robot. For input, we take the RGB images for the two cameras equipped on the robot head and wrist separately. The head camera provides an overview of the workspace while the gripper camera offers a close observation of the interaction area between the end effector and the environment.

We fine-tune Octo-Base, OpenVLA, and KosMos P.H. built by RoboVLMs on the real robot benchmark and compare their performance. The result is shown in Fig. 4d. We observe that the best VLA (KosMos P.H.) built by RoboVLMs achieves the best performance in all evaluation setups, especially on *Simple* and *Unseen Background*, demonstrating their effectiveness and generalization ability, which is consistent with the results in *SimplerEnv* and CALVIN simulation.

The qualitative results are shown in Appendix, including success rollouts in various settings and some representative failure cases. KosMos P.H. not only outperforms baseline models in basic setting tasks like *Open Drawer*, *Pickup Eggplant* and *Press the Toaster Switch*, but also achieves better performance over unseen objects, distractors, and backgrounds. Furthermore, as shown in Extended Fig. 1, KosMos P.H. emerges with self-correction ability, it can realize the incorrect positions of the end effector and correct its future trajectory to complete the task successfully. Note that this ability does not appear in the other tested baselines, and this kind of data is not contained in the training dataset.

Finding 1.2: The best setup VLA built by RoboVLMs appears to have strong effectiveness and robustness in real scenarios.

In the following, we will explain our empirical studies and corresponding findings in detail, including the settings, results, and takeaways in building VLAs from pre-trained VLMs.

C. Which kind of VLM backbones are suitable for VLAs?

When building a VLM-based VLA, the first question is which VLM backbone is the most appropriate one for our VLA:

Question 2: Which type of VLMs is most suitable for constructing VLAs?

To thoroughly investigate this question, it would be ideal to conduct experiments in highly controlled settings. However, training VLMs on large-scale vision-language datasets is extremely resource-intensive. Therefore, we base our VLAs on a diverse set of off-the-shelf, pre-trained, large-scale vision-language backbones with varying architectures, training data scales, model sizes, and latent embeddings. These include Flamingo model family [1] (Encoder-Decoder), and a series of decoder-only VLMs, including LLaVA [26], Qwen-VL [2], MoonDream [42], UForm [40], Paligemma [3], and KosMos [34]. Noticeably, in this section, for fair comparisons, all the models are trained with static images instead of both static and hand cameras.

TABLE I: The ablation study on CALVIN benchmark over the effect of action space, history integration, and history organizing format. All variants are trained on split ABCD and tested on split D. ‘‘Disc.’’ is short for discrete and ‘‘Cont.’’ represents continuous action space. Note that for VLAs with LLaVA backbone, we utilize a perceiver resampler to downsample its vision tokens to 64 for fair comparison. Results are reported with models trained maximally within 5 epochs on the ABCD training splits, all structures predict an action chunk with size 10 and only execute the first step action for inference.

Backbone	Structure	Action Space	Consecutive tasks success rates					Avg. Len.
			1	2	3	4	5	
LLaVA	One-Step	Disc.	0.809	0.484	0.278	0.175	0.103	1.85
	One-Step	Cont.	0.793	0.592	0.420	0.329	0.235	2.37
	Interleaved	Cont.	0.892	0.645	0.436	0.282	0.181	2.44
	Policy-Head	Cont.	0.873	0.678	0.506	0.376	0.275	2.71
Flamingo	One-Step	Disc.	0.681	0.318	0.133	0.062	0.029	1.22
	One-Step	Cont.	0.681	0.354	0.158	0.076	0.035	1.30
	Policy-Head	Cont.	0.964	0.896	0.824	0.740	0.662	4.09
KosMos	One-Step	Disc.	0.424	0.097	0.023	0.005	0.002	0.55
	One-Step	Cont.	0.935	0.868	0.814	0.768	0.702	4.09
	Interleaved	Cont.	0.987	0.915	0.824	0.737	0.660	4.12
	Policy-Head	Cont.	0.967	0.930	0.899	0.865	0.826	4.49
PaliGemma	One-Step	Disc.	0.316	0.096	0.021	0.005	0.001	0.44
	One-Step	Cont.	0.933	0.863	0.808	0.751	0.688	4.04
	Interleaved	Cont.	0.949	0.896	0.851	0.803	0.754	4.25
	Policy-Head	Cont.	0.984	0.933	0.888	0.835	0.779	4.42

The results, presented in Extended Table. 5, reveals the following observation: KosMos and Paligemma demonstrate the distinctively better performance. From Extended Table. 5, we can see that these two backbones are much better than others with a significantly clear margin. Their superior performance benefits from sufficient vision-language pre-trained on large vision-language datasets. This outcome is intuitive, as extensive pretraining facilitates stronger alignment between visual and linguistic features, an alignment critical for language-conditioned manipulation tasks.

Finding 2: VLAs benefit from sufficient vision-language pre-training on larger vision-language datasets of VLMs backbone.

D. How should VLAs be formulated to best leverage VLMs?

In this section, our study addresses questions regarding VLA formulations, including different design choices of VLA structures and various backbones. To answer these questions, we conduct a series of controlled experimental studies to evaluate various VLA formulations on the CALVIN benchmark for rapid evaluation.

Question 3.1: How to select the best-performing VLA structure?

More specifically, how should we model observations, states, and actions in robot manipulation tasks within the context of a VLA? To explore this question, we implement several variants, leveraging various open-source VLM backbones such as OpenFlamingo [33], LLaVA [26], and KosMos [34]. These variants incorporate different historical information modeling strategies, and action spaces, as discussed and categorized in Sec.I.

The performance of various VLA structures in CALVIN is summarized in Table. I. From these results, we draw the following key observations:

- **Continuous action matters:** By comparing two types of action spaces, **continuous** and **discrete**, as shown in Table. I, we observe that under the single-frame formulation, continuous action spaces consistently outperform discrete ones, particularly as task horizons increase. This finding is intuitive: continuous actions can represent high-precision floating-point values, whereas discrete actions are limited to indexing action intervals. For long-horizon tasks, the accumulation of compounding errors significantly degrades the performance of discrete actions.
- **History observation matters:** As shown in Table. I, under the same VLM structure (either Encoder-Decoder or Decoder-only), models incorporating history observations as input consistently outperform one-step models, achieving substantially higher success rates across all tasks. This improvement holds regardless of the history fusion strategy used. Furthermore, increasing the length of an observable history can enhance performance, albeit at the cost of higher computational overhead.
- **Policy head improves history fusion:** Among the formulations utilizing history, the interleaved history formulation performs worse than merging history via an additional policy head. We hypothesize that the policy head preserves the VLM’s original vision-language fusion capabilities while effectively integrating historical information. Moreover, the

interleaved formulation incurs significantly higher memory and FLOP costs during both training and inference. This suggests that incorporating history with an additional policy head is a more effective and efficient approach for VLAs.

Finding 3.1: The VLA achieves its best performance when using multi-step historical observations as inputs and continuous actions as outputs. For integrating history with continuous action space, the policy head structure performs better.

However, beyond the performance itself, one of the most important challenges for modern VLAs is achieving generalization to novel objects and environmental settings, which is critical for practical deployment across various robots and scenarios. Conversely, when generalization is insufficient, fine-tuning the policy with a few new demonstrations becomes ideal. Thus, VLAs should inherit the generalization capabilities of VLMs in open-world settings while maintaining high data efficiency when additional in-domain training samples are available.

Therefore, we further investigate the generalization and data efficiency for different VLAs formulations.

Question 3.2: How do different formulations affect the generalization and data efficiency for VLAs?

To address the question, we empirically study and evaluate the generalization and data efficiency of various VLA formulations, aiming to provide practical insights for training high-performing VLAs. Specifically, we assess the generalization and data efficiency of different VLAs built with RoboVLMs by training models with different architectures and formulations on varying data scales using the CALVIN datasets. As discussed earlier, we focus on comparing the interleaved and policy head formulations using the OpenFlamingo and KosMos backbones, which have shown strong potential among all configurations. Note that the interleaved formulation can only be paired with a decoder-only structure. The results presented in Fig. 4c and Extended Table 4, lead to the following observations:

- **For generalization performance** (Fig. 4c), our best model, based on the KosMos backbone and leveraging a policy head for history fusion, exhibits only a slight performance drop in zero-shot settings. In contrast, other formulations experience significant performance declines. This finding highlights that the model architecture significantly impacts generalization. This conclusion is further supported by results in Fig. 4a, where tasks in the evaluation set are paired with novel instructions, and Fig. 4d, where our best model outperforms others by a large margin across all unseen tasks.
- **For data efficiency**, we observe trends similar to those for generalization. Our best model consistently achieves the highest performance when training data is scaled down, with a notably slower performance decline compared to other formulations. Additionally, comparisons of encoder-decoder VLAs at different scales reveal that larger models tend to be more data efficient.

Finding 3.2: Leveraging policy head for history fusion is the best in terms of generalization and data efficiency.

Yet, the historical formulation is demonstrated to have the best performance, most recent learning-based techniques favor the one-step-continuous formulation for its computational efficiency, with an acceptable performance drop on short-horizon tasks. This offers a practical trade-off, particularly for real-robot deployment [4, 20]. To further investigate their impacts on the performance of resulting policies, we based them on the state-of-the-art one-step-continuous formulation with the best-performing PaliGemma backbone, to align with their original backbone setting and ensure fair comparison.

Question 3.3: How do training objectives and inference-time aggregation strategies impact the performance?

Learning-based policies vary in training objectives and inference, leading to different execution behaviors. For example, in behavior cloning, the most prevailing way is to use MSE or BCE losses for action generation, while diffusion policies learn denoising trajectories through generative modeling. We investigate different training objectives along with the widely-exploited inference-time aggregation strategies for a comprehensive understanding.

In detail, we compare the following two objectives, which are the most prevailing ones in current days:

- **Flow Matching [4, 24]** is a diffusion-based objective. It regards the denoising process as a continuous flow and samples timestep $t \in [0, 1]$ to enforce the model to predict the velocity at t . For inference, the model randomly samples an action-chunk shaped gaussian noise, and predicts the denoising velocity based on the current action chunk and time step, the denoised velocity is added to the action chunk vector until the maximum denoising step is reached.
- **MSE+BCE [22, 45]**. It formulates the action as an $n + 1$ -dimensional vector, with n continuous actions representing arms or end-effector poses, plus a separate gripper action. It utilizes Mean Square Error (MSE) to learn the continuous actions and Binary Cross Entropy (BCE) to learn the state of the gripper.

Besides, we also compare different inference-time action aggregation strategies including *Chunk*, *First*, and *Ensemble*:

- **Chunk:** A chunk will be fully executed before the next inference.
- **First:** Only the first action in the chunk will be executed, and then run the next inference.

TABLE II: The performance of VLAs with different training objectives and action execution paradigms, and whether to introduce the MoE structure. We utilize PaliGemma, which aligns with the settings of π series, as the VLM backbone and implement Fully Connecting (FC) with MSE and Flow Matching (FM) loss. Note that the FC with Flow Matching loss and MoE structure is identity with π_0 , and for fair comparison, we do not consider state as input. For executing paradigms, we verify three different paradigms: **Chunk** represents that the VLAs execute the entire chunk. **First** refers to VLAs execute the first action in the chunk. **Ensemble** refers to ensemble the first action with the corresponding actions in history chunks.

(a) Performance with different training objectives and execution paradigms

Training Objective	Training Split	Executing Paradigm	Consecutive tasks success rates					Avg. Len.
			1	2	3	4	5	
Flow Matching	ABC	Chunk	0.910	0.812	0.730	0.652	0.573	3.68
Flow Matching		First	0.793	0.586	0.442	0.351	0.273	2.45
Flow Matching		Ensemble	0.838	0.710	0.614	0.545	0.437	3.14
MSE+BCE		Chunk	0.901	0.802	0.703	0.620	0.544	3.57
MSE+BCE		First	0.822	0.564	0.371	0.265	0.169	2.19
MSE+BCE		Ensemble	0.880	0.730	0.606	0.508	0.414	3.14
Flow Matching	ABCD	Chunk	0.937	0.872	0.811	0.764	0.705	4.09
Flow Matching		First	0.898	0.799	0.701	0.618	0.544	3.56
Flow Matching		Ensemble	0.945	0.882	0.818	0.770	0.708	4.12
MSE+BCE		Chunk	0.933	0.863	0.808	0.751	0.688	4.04
MSE+BCE		First	0.925	0.727	0.579	0.473	0.378	3.06
MSE+BCE		Ensemble	0.925	0.849	0.784	0.721	0.664	3.94

(b) Effectiveness of Mix-of-Expert structure

Training Objective	Using MoE	Consecutive tasks success rates					Avg. Len.
		1	2	3	4	5	
MSE+BCE	✓ (ABC)	0.932	0.824	0.732	0.644	0.556	3.69
MSE+BCE	✗ (ABC)	0.901	0.802	0.703	0.620	0.544	3.57
Flow Matching	✓ (ABC)	0.940	0.855	0.768	0.679	0.597	3.84
Flow Matching	✗ (ABC)	0.910	0.812	0.730	0.652	0.573	3.68
MSE+BCE	✓ (ABCD)	0.945	0.823	0.678	0.561	0.457	3.46
MSE+BCE	✗ (ABCD)	0.933	0.863	0.808	0.751	0.688	4.04
Flow Matching	✓ (ABCD)	0.911	0.828	0.759	0.707	0.639	3.84
Flow Matching	✗ (ABCD)	0.937	0.872	0.811	0.764	0.705	4.10

- **Ensemble**: An ensemble strategy [51] is used to aggregate the predictions at the same time step from different action chunks.

From Table. IIa we could observe that:

- **Diffusion policies do not significantly improve performance compared to MSE+BCE**. While Flow Matching slightly outperforms MSE+BCE in all experiments, the performance gap is not significant. This suggests that the added inference-time complexity of diffusion models offers limited benefit for short-horizon tasks where deterministic objectives already perform well.
- **One-Step-Continuous policies benefit most from executing full action chunks**. Across both Flow Matching and MSE+BCE, the Chunk paradigm consistently yields the best performance in novel scenarios (Training Split ABC). This is likely because the models learn to generate trajectories from a multimodal distribution, and executing only the first action or aggregating across chunks (as in Ensemble) can introduce mode collapse or distort the intended trajectory. Chunk execution preserves temporal coherence within the sampled sequence. While in seen scenarios (Training Split ABCD), executing action chunks does not achieve significant performance improvement compared with ensembling. This indicates that in seen scenarios, the diversity of trajectories might be decreased so that executing action chunks is comparable with ensembling. However, chunking execution could decrease the inference times of VLAs and achieve a real-time deployment (over 30HZ), so that for the rest of the experiments, we utilize chunking execution for one-step-continuous policies.
- **Executing only the first action underperforms across both objectives**. The First paradigm results in significantly lower performance regardless of training objective, especially as the sequential task progresses. This suggests that relying solely on the first action from a sampled or predicted sequence lacks the temporal context and consistency, which are particularly necessary for long-horizon task success.

Finding 3.3: For One-Step-Continuous formulation, Diffusion loss and MSE loss could achieve a similar performance. For inference-time aggregation strategy, it is important to keep execution consistency, particularly for long-horizon tasks and multimodal actions.

Inspired by the Mixture-of-Experts (MoE) in deep learning [37], which dynamically routes inputs through specialized feed-forward networks, π_0 [4] proposes augmenting each VLM layer with a dedicated action expert. This design, used in the π_0 [4] and $\pi_{0.5}$ [15] series, preserves vision-language reasoning by routing vision and language tokens through the original VLM modules, while action tokens are handled by the expert and fused via self-attention. Given its demonstrated effectiveness, we also investigate the impact of this structure under our policy formulation.

Question 3.4: Does Mix-of-Expert structure benefit VLA learning?

To assess the effectiveness of the MoE design, we adopt the same setup as the π -series as shown in Extended Fig. 2b, where the vision-language (VL) tokens are processed by the standard VLM feedforward network (FFN), and the action tokens are routed through a separate action expert FFN. The two sets of tokens interact via self-attention, maintaining joint reasoning while allowing specialization. We evaluate this structure under two representative training objectives: MSE+BCE and Flow Matching, which follow both our default settings in this paper and the original setting in π -series, respectively.

From Table. IIb, we observe that

- MoE structure consistently improves generalization in the visually zero-shot setting (Training Split ABC). For both MSE+BCE and Flow Matching training objectives, using MoE yields higher success rates across all five consecutive tasks. This suggests that MoE enhances the model’s ability to generalize to unseen scenarios. This demonstrates that the mixture-of-experts (MoE) structure is beneficial in preserving the pretrained vision-language (VL) capabilities, as the action prediction does not impose strong supervision on the visual tokens.
- For seen scenarios (Training Split ABCD), introducing the MoE structure does not provide additional benefits. Both training objectives achieve higher success rates without MoE, suggesting that for scenes similar or identical to the training data, the original VLM backbone is sufficient. This may originate from that the MoE structure tends to preserve the general pretrained vision-language (VL) representations, whereas directly fine-tuning the VLA backbone without MoE allows the model to specialize instead of generalize, and fit more effectively to the seen tasks, leading to better performance under familiar settings.

Finding 3.4: Introducing the Mix-of-Expert structure can improve the generalization of VLAs, while it can not boost the performance in seen scenarios.

E. When should we leverage the public diverse robot data for optimal training?

In recent work, it has been a dominant trend to leverage large-scale cross-embodiment robot manipulation datasets to improve the performance of VLAs [4, 7, 20, 33]. However, it is still not fully clear if it helps and an important question remains:

Question 4: How do large-scale cross-embodiment datasets contribute to VLAs?

To address this, we break the question into two sub-questions:

- 1) What types of data from large-scale cross-embodiment datasets are the most beneficial for building VLAs?
- 2) When and how should these data be utilized effectively?

In this section, we conduct a series of experiments to investigate different strategies for using external large-scale cross-embodiment datasets. Specifically, we explore three settings as shown in Extended Fig. 3:

- **Co-train:** Training the model with in-domain manipulation data and cross-embodiment datasets. Previous work like RT-2 [7], OpenVLA [20], and OCTO [38] only consider this one-stage training.
- **Post-train:** First, Co-training the VLMs on in-domain and cross-embodiment datasets as above; then, fine-tuning with in-domain manipulation tasks. This has been adopted by π_0 [4].
- **Finetune:** Without involving cross-embodiment datasets, fine-tuning the model with only in-domain manipulation tasks. For RT1 dataset that includes the exact target tasks, we further split the RT1 dataset into target tasks and extra in-domain data.

Our experiments in this section use the best-performing KosMos backbone with a policy head for history fusion as the base model. We use Open X-Embodiment (OXE) [33] as the cross-embodiment dataset, which comprises a diverse range of robot manipulation data collected worldwide and is the most widely used one in recent works [4, 7, 20, 38].

D.1 In Domain Evaluation

We first test on the general in-domain tasks (i.e., tasks inside OXE). For comparison, we also evaluate a baseline setting, **Finetune**, where the VLA is trained exclusively on in-domain data. Additionally, for **Google Robot**, we include both *RT-Partial*

Finetune and *RT Finetune*, where *RT-Partial Finetune* involves only the trajectories with the same task type as the evaluating tasks, and *RT Finetune* involves co-finetuning the policy with additional data from the same robot across different tasks. For *Bridge*, we only evaluate *Bridge Finetune*, which finetunes the policy with the entire *Bridge-V2* dataset, since the training dataset does not contain trajectories with the same instructions as the evaluated tasks.

The comparison of the two stages of using cross-embodiment data is shown in Extended Fig. 4, showing the evaluation results for **SimplerEnv-*Google Robot*** and **SimplerEnv-*Bridge***, from which the following observations can be drawn:

- **Co-training on cross-embodiment data without post-training does not help significantly.** Comparing *OXE Co-train* and *RT-Partial Finetune* reveals that for both *Google Robot* and *Bridge*, co-training with cross-embodiment data does not lead to substantial performance improvements. In particular, for *Google Robot*, training with additional in-domain data (*RT Finetune*) from different tasks achieves higher success rates (compared with *RT-Partial Finetune*). This indicates that in-domain data, even if task-agnostic, is more effective for improving model performance than cross-embodiment data.
- **Post-training shows potential benefits over high-frequency tasks in the first co-training stage.** The average performance of the post-trained model exceeds that of the model fine-tuned exclusively on in-domain data on *Bridge* (50% for post-trained and 44% for fine-tuned). While for *Google Robot*, the post-trained model only outperforms the fine-tuned model over `pick coke can` tasks, and drops its performance on all other tasks. We consider the main reason is that the proportion of `pick-and-place` tasks in the OpenX-Embodiment dataset is very large, so that the post-trained model gains higher performance over `pick-and-place` tasks, while it loses performance over tasks involving other skills like `move near` and `open/close drawer` as a trade-off. In other words, cross-embodiment co-training enables VLAs to learn skills for high-frequency tasks from other types of embodiments and transfer the acquired knowledge to the target embodiment during the post-training phase. This helps VLAs further improve the overall success rate of these tasks, though at the cost of sacrificing low-frequency tasks and skills in the co-training stage.
- **In-domain data plays a critical role in achieving strong task performance.** Even task-agnostic in-domain data from the same embodiment (e.g., *RT Finetune*) proves more effective than large-scale cross-embodiment data for fine-tuning VLAs, as shown by the experiments on *Google Robot* dataset, especially for fitting specific tasks. While cross-embodiment pre-training can provide useful initialization in some cases, leveraging in-domain data remains essential for robust and consistent policy performance.

D.2 Out-of-Distribution Evaluation

To evaluate the impact of cross-embodiment datasets more comprehensively, we further perform experiments on **CALVIN**, whose data is not part of OXE. We mainly focus on whether cross-embodiment datasets benefit **few-shot learning** (we randomly sample 10 trajectories for each task from data split ABCD for training and test on D) on out-of-distribution tasks (w.r.t. to OXE). To keep settings consistent, we only take the image from the static on-head camera as input. The results are illustrated in Extended Fig. 5, and we conclude that:

- **Cross-embodiment pre-training improves few-shot learning performance.** In the few-shot setting for CALVIN, with a single-view on-head camera, pre-training significantly improves the performance by 17.2% in terms of single-task execution and 0.25 more executed tasks in each rollout. It can be concluded that pre-training on large-scale cross-embodiment datasets benefits the learning of more effective representations for robot manipulation, which can quickly adapt to novel manipulation tasks with unseen objects and environmental settings.

Finding 4: Extra in-domain data, even from different tasks, shows beneficial, and an extra large-scale cross-embodiment co-training before the post-training stage further improves high-frequency tasks as well as few-shot performance.

III. METHOD AND MATERIAL

We consider the problem of controlling a robot to accomplish a set of tasks, based on language instructions l , and historical observations $o_{t-H+1:t}$ at every time step t with the maximum historical length H . In this paper, we mainly consider a table-top robot arm, therefore the observations o_t are sensor inputs and images, e.g., $o_t = (s_t, I_t)$, from either a third-view camera, a gripper camera, or both. We build a controlling policy $\pi(a|o_{t-H+1:t}, l)$, where the action a is modeled as a 7-dim vector, including the 6-DoF pose of the gripper, along with its open/close status. In this section, we will first introduce the formulation of vision-language models (Section III-A), based on which we build our VLA formulations.

A. Vision Language Model

Vision-language models (VLMs), also referred to as multi-modal large language models, integrate vision into their input modality, enabling them to process and reason about both visual and textual information. Typically, VLMs are prompted with images and/or text to generate text [1, 2, 3, 26, 40, 42], facilitating applications such as image captioning, visual question answering, and goal-directed planning. This process can be formally described as:

$$\hat{l} = \text{VLM}(I, l_{\text{prompt}}) . \quad (1)$$

Here, I and l_{prompt} denote the image and text prompts, respectively, while \hat{l} represents the text output generated by the VLM. For instance, in a visual question-answering task, l_{prompt} corresponds to the question, and l_{target} corresponds to the generated answer. Training a VLM typically involves minimizing a cross-entropy loss to predict discrete language tokens, which can be expressed as:

$$\ell_{\text{VLM}} = \text{CrossEntropy}(\hat{l}, l_{\text{target}}) , \quad (2)$$

where l_{target} is the ground truth text. By pre-training on millions or even billions of paired vision-language data, VLMs acquire robust representations of both visual and textual modalities. To effectively handle these two distinct modalities, VLMs typically employ a vision processor and a language decoder, connected through various vision-language feature fusion mechanisms. Among the available options, vision transformer (ViTs) [11] and perceiver resampler [16] are widely adopted choices for the vision processor [22, 28, 38, 45]. The ViT module reshapes each input image I into patches and encodes them as visual tokens [OBS]:

$$[\text{OBS}] = (x_1^v, \dots, x_N^v) = \text{ViT}(I) , \quad (3)$$

where N represents the token number, x_i^v represents the i th token, which, in ViT, is an embedding vector encoding a patch of the input image.

Existing VLMs can be broadly categorized into two structural paradigms: encoder-decoder and decoder-only architectures. These two structures differ mainly in their multi-modal fusion strategies.

Encoder-decoder. Encoder-decoder architectures are composed of two main components: an encoder that is typically responsible for extracting features from inputs using input embedding modules as discussed above, and a decoder that generates the output (e.g., text or multi-modal predictions) auto-regressively. Feature fusion between the encoder and decoder is usually achieved by cross-attention layers in the decoder. This structure excels in tasks requiring a detailed understanding of the input modalities, such as image captioning and visual reasoning, due to its ability to explicitly encode multi-modal information prior to generation [31, 46]. Representative models include Flamingo [1] and OFA [44].

Decoder-only. Decoder-only architectures, in contrast, rely on a unified transformer framework where both the input modalities (vision and text) and the output sequences are processed in the same autoregressive decoder. In these models, visual features are first embedded into token-like representations (via vision processors), which are then concatenated with textual tokens and passed through the decoder. Multi-modal feature fusion occurs naturally through the self-attention mechanism, allowing the decoder to model dependencies between visual and textual inputs during token generation. Decoder-only architectures are more flexible and scalable, making them well-suited for tasks like instruction following, multi-modal question answering, and open-ended generation. Examples of decoder-only models include GPT-4V [47] and LLaVA [26].

B. Vision-Language-Action Models

Vision-language-action models (VLAs) are predominantly applied to robotic tasks, where they serve as a generalist robot policy π capable of handling complicated tasks. In formal, VLAs predict action sequences based on previous observations at the current time step t :

$$a_{t:t+L-1} = \text{VLA}(o_{t-H+1:t}, l_{\text{prompt}}) , \quad (4)$$

where $a_{t:t+L-1}$ are a sequence of predicted 7-dim actions, L is the action sequence length and H is the history observation length. Different from VLMs, the observations of VLAs $o_{t-H+1:t}$ usually contain proprioceptive states $s_{t-H+1:t}$ like the joint angles and end-effector positions besides the visual inputs $I_{t-H+1:t}$. As discussed in Section III-B, we abstract and categorize VLAs into four representative structures based on 1) historical information modeling and 2) action space. Before we describe these distinct models in form, we first introduce the general pre-process and prediction principles when dealing with robot actions in different action spaces.

1) Action Pre-process

Action Normalization. For both continuous and discrete action spaces, we normalize each dimension of the 7-DoF action. Following Kim et al. [20], we count the 1st and 99th quantile of the actions in the training data and use the quantiles to clamp each dimension of the action [7]:

$$a^{i'} = \min(a_{99\text{th}}^i, \max(a_{1\text{st}}^i, a^i)) , \quad (5)$$

where $a^{i'}$ is the clamped value of the i -th dimension of action a . For the next step, we normalize each dimension of the clamped action a' with the 1st and 99th quantile of the actions:

$$\tilde{a}^i = 2 \times (a^{i'} - a_{1\text{st}}^i) / (a_{99\text{th}}^i - a_{1\text{st}}^i) - 1 . \quad (6)$$

$\tilde{a} = [\tilde{a}^1, \tilde{a}^2, \dots, \tilde{a}^7]$ is the normalized action, each dimension is in the range of $[-1, 1]$, the last dimension representing the open/close status of the gripper $\in \{-1, 1\}$. During inference time, we will reversely map the predicted actions into unnormalized actions.

Action Discretization. For discrete action representation, we need to further discretize the normalized action \tilde{a} . Following Brohan et al. [7], Kim et al. [20], we map continuous robot actions to discrete tokens used by the VLM's tokenizer. Specifically,

we discretize each robot action dimension into one of 256 bins separately. For each dimension, we set the width of the bin to uniformly divide the interval between the quantile of 1st and 99th of actions in the training data.

Using this discretization, we transform \tilde{a} to \bar{a} with 7 discrete integers $\in [0 \dots 255]$. To avoid damaging the original special token positions in the language tokenizer, we add an offset (default set to 10) and replace the last offset $\sim 256 + \text{offset}$ tokens with a discretized index.

2) **Action Prediction Continuous Actions.** We optimize the mean square error (MSE) and binary cross entropy (BCE) for the predicted action sequence $a_{t:t+L-1}$ with the ground truth action sequence $\tilde{a}_{t:t+L-1}$:

$$l_{\text{VLA}} = \sum_{i=t}^{t+L-1} \text{MSE}(\hat{a}_{i,\text{pose}}, \tilde{a}_{i,\text{pose}}) + \lambda * \text{BCE}(a_{i,\text{gripper}}, \tilde{a}_{i,\text{gripper}}), \quad (7)$$

where the MSE loss is computed for the first six dimensions, and the BCE loss is for the last gripper dimension between the predicted action $\hat{a}_{t:t+L-1}$ and the ground truth $\tilde{a}_{t:t+L-1}$, λ is the balancing weight.

Discrete Actions. Discrete-action models predict action tokens ACT^i for each action dimension i . These tokens are the index of discretized bins from continuous action by dimension, which can be easily de-tokenized to recover the action vector. The optimization object has a similar cross-entropy (CE) format as text generation widely used in VLM training:

$$l_{\text{VLA}} = \sum_{i=t}^{t+L-1} \sum_{j=1}^7 \text{CE}([\text{ACT}]_i^j, \tilde{a}_i^j), \quad (8)$$

where $[\text{ACT}]_i^j$ represents the index of bins of the j^{th} dimension of the predicted action token $[\text{ACT}]$ at time i , and \tilde{a}_i^j is the corresponding ground truth. During inference time, after getting the predicted action token ACT^i , we re-project the discrete tokens to the center of the corresponding bins into a continuous form for achieving tasks.

C. VLA Structures

As shown in Extended Fig. 2a, there are mainly four kinds of VLA structures categorized by action space and history aggregating method, namely one-step-continuous-action models, one-step-discrete-action models, interleaved-continuous-action models, and policy-head-continuous-action models. Note that our proposed framework RoboVLMs could transfer VLMs to arbitrary VLA structures with no effort. We will illustrate the four VLA structures in detail in the following section. 1) *One-step Models* One-step models predict future action sequences using only the observation at the current time step t , i.e., a history length of 1.

$$\hat{a}_{t:t+L-1} = \text{VLA}(o_t, l_{\text{prompt}}). \quad (9)$$

For one-step models, we formulate two variants: continuous-action model and discrete-action model:

Continuous-action model: In the continuous-action formulation, the VLM model first predicts a learnable token $[\text{LRN}]$ using the VLM backbone. This is achieved by fusing visual and language tokens (in an encoder-decoder architecture) or concatenating multi-modal tokens (in a decoder-only architecture). An MLP is then used to predict the action vector:

$$\begin{aligned} [\text{LRN}] &= \text{VLM}(o_t, l_{\text{prompt}}), \\ \hat{a}_{t:t+L-1} &= \text{MLP}([\text{LRN}]). \end{aligned} \quad (10)$$

The one-step continuous-action models include ACT [51], BC-Z [17], MVP [35], R3M [32], VIMA [18], 3D Diffuser [19], RoboMamba [28], and π_0 [4].

Discrete-action model: For discrete action prediction, we directly follow the straightforward next-word prediction similar to VLMs, where actions are discretized into tokens like texts:

$$[\text{ACT}]_{t:t+L-1}^{1:7} = \text{VLM}(o_t, l_{\text{prompt}}). \quad (11)$$

The one-step discrete-action models include RT-1 [6], RT-2 [7], 3D-VLA [53], LAPA [48], OpenVLA [20], and Embodied-COT [50].

2) *Interleaved-Continuous-Action Models* Interleaved models receive observation-action sequences:

$$O_t = ([\text{OBS}]_{t-H+1}, [\text{LRN}]), \dots, ([\text{OBS}]_t, [\text{LRN}]), \quad (12)$$

where O_t represents the input token sequence at time instant t , $[\text{OBS}]$ denotes observation tokens and $[\text{LRN}]$ denotes the learnable action token and is duplicated for H times and insert into O_t with an interleaved format. The VLM backbone fuses this sequence (in a decoder-only structure) and predicts the action sequence through an MLP based on each action token:

$$\begin{aligned} [\text{LRN}]_{t-H+1:t} &= \text{VLM}(O_t), \\ \hat{a}_{t:t+L-1} &= \text{MLP}([\text{LRN}]_t). \end{aligned} \quad (13)$$

The $[\text{LRN}]_t$ which is utilized to predict the action chunk $\hat{a}_{t:t+L-1}$, represents the $[\text{LRN}]$ inserted after $[\text{OBS}]_t$ and fused with the observations before t . The loss and action unnormalization procedure is identical with one-step continuous action

models. At time instant t of inference, the input sequence contains only the current observation $[\text{OBS}]_t$ and the language instruction l_{prompt} , we add the learnable token $[\text{ACT}]$ at the end of the input sequence and pass the sequence to the VLM to predict the action. After the robot executes the predicted action, we add the new observation $[\text{OBS}]_{t+1}$ and language instruction l_{prompt} to the input sequence to predict the action in the current step. The interleaved-continuous-action models include GR-1 [45], OCTO [38], GR-2 [8]. Note that the interleaved-discrete-action models like GATO [36] and RoboCat [5] are out of consideration.

1) *Policy-Head-Continuous-Action Models*: Unlike interleaved models, which fuse historical information within the VLM backbone, policy-head VLAs only require the VLM to provide single-step multi-modal representations at each time step t :

$$\begin{aligned} o_t &= ([\text{OBS}]_t, [\text{LRN}]) , \\ [\text{LRN}]_t &= \text{VLM}(o_t, l_{\text{prompt}}) . \end{aligned} \quad (14)$$

Historical information is then modeled and actions are predicted through an additional policy head h , such as an RNN [10, 14, 29], transformer [13, 41], or diffusion model [9]:

$$a_{t:t+L-1} = h([\text{LRN}]_{t-H+1}, \dots, [\text{LRN}]_t) . \quad (15)$$

The action chunk $a_{t:t+L-1}$ with sequence length L is predicted based on learnable tokens $[\text{LRN}]_{t-H+1}, \dots, [\text{LRN}]_t$. Each of $[\text{LRN}]_t$ is identical. Note that the interleaved-continuous-action model is only available for decoder-only backbones. The policy-head-continuous-action model can be built based on VLM backbones with both encoder-decoder and decoder-only structures. The main difference comes from the language decoder. The input sequence of the encoder-decoder VLM fuses only contains the text and learnable action tokens, it fuses the multi-modal input with cross-attention where the text tokens combined with the learnable tokens are the keys and values, and vision tokens are the queries. The decoder-only backbone directly concatenates the vision, language, and learnable tokens as input and utilizes self-attention to fuse the multi-modal features. The policy-head-continuous-action models include RoboFlamingo [22], RoboUniview [25], and DeerVLA [49].

At every inference step t , the current observation $[\text{OBS}]_t$ and language instruction l_{prompt} along with a learnable token $[\text{LRN}]$ is concatenated as a complete input sequence, which is further passed into the VLM backbone. After the policy head takes $[\text{LRN}]$ and predicts the current action sequences, the robot steps with the predicted actions and obtains the new observation for the next round of prediction.

D. Real Robot Platform

As shown in Fig. 3b, our real robot platform consists of a Kinova Gen-3 robot arm, equipped with a Robotiq 2F-85 parallel-jaw gripper and two cameras: one static camera for capturing the workspace and another camera mounted on the end-effector. The static camera is a Kinect Azure, while the wrist-mounted camera is a RealSense D435i. The workspace is a 55 cm x 24 cm table, and there are more than 40 objects distributed across the evaluated scenes.

As described in Section II, we define one simple setting and four unseen settings for evaluation on this platform. For the convenience of readers, we provide a more detailed introduction to these settings here. In the *Simple* setting, the scene is designed to closely resemble those in the training data. This setting is used to assess the model’s ability to fit the training distribution. In the *Unseen Distractors* setting, previously unseen distractor objects are introduced into the scene, but the manipulated objects are still part of the training data. The *Unseen Backgrounds* setting changes the background by adding two new tablecloths that were not present in the training data. One tablecloth differs in color from the white background, while the other features entirely different patterns. In the *Unseen Objects* setting, the robot is tasked with manipulating objects that were not included in the training dataset. The unseen objects used in this setting are the same as those in the Unseen Distractors setting. Finally, in the *Novel Skill Description* setting, we use GPT-4 to generate three unseen synonyms for the verbs in the instructions and randomly select one to replace the original verb, creating a novel skill description. For instance, "press" may be replaced with "hit," "pick up" with "take," "close" with "shut," "pour" with "sprinkle," and so on.

E. Discussions about Structures

Although we have discussed four representative VLA structures, by a two-level categorization of historical information and action space, readers may notice that these two dimensions are not entirely orthogonal, and not all combinations are discussed and implemented in this work. This is due to architectural limitations and implementation challenges. For instance, interleaved and policy-head models with discrete action spaces have not been implemented so far, because interleaved models are typically combined with action chunk prediction, where the default lower triangular attention mask cannot effectively mask subsequent actions for later steps.

IV. DATA AVAILABILITY

Datasets used in this study could be found at <https://github.com/mees/calvin> (CALVIN), https://github.com/google-deepmind/open_x_embodiment (Open X-Embodiment), and https://huggingface.co/datasets/robowlms/bytedance_robot_benchmark_20 (BDRBench20).

V. CODE AVAILABILITY

The source code of this study could be found at <https://github.com/Robot-VLAs/RoboVLMs>. It is also available at <https://zenodo.org/records/17757179> [?].

VI. ACKNOWLEDGMENTS

This work was supported in part by the National Natural Science Fund under Grant 62025304 and in part by the National Natural Science Fund for Key International Collaboration under Grant 62120106005. We thank all the members of the robotics research team at ByteDance Research for their assistance in real-world data collection, setup design, robot maintenance, and experiments. The author Minghuan Liu is supported by the ByteDance Scholarship. We also want to thank @YouJiacheng for his active and instructive discussion on X.

VII. CONTRIBUTIONS

Project Leads: Huaping Liu, Xinghang Li, Hanbo Zhang, Minghuan Liu

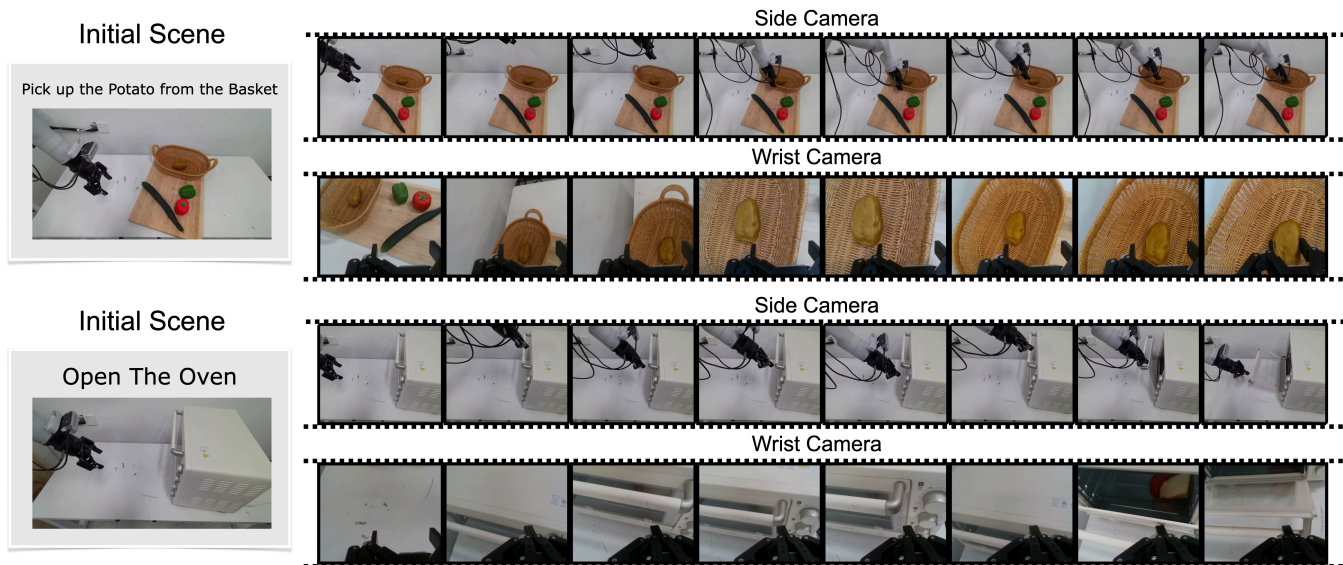
Methodology and Codebase: Xinghang Li

Model Training and Evaluation (experimental design, implementation): Xinghang Li, Long Qian, Hanbo Zhang, Dong Wang, Minghuan Liu, Xiao Ma, Jirong Liu

Real-Robot Deployment & Experiments: Xinghang Li, Peiyan Li

Paper (logic, figures, visualizations, writing): Xinghang Li, Minghuan Liu, Hanbo Zhang, Long Qian, Bingyi Kang, Xiao Ma, Peiyan Li, Jirong Liu, Di Guo, Huaping Liu, Tao Kong

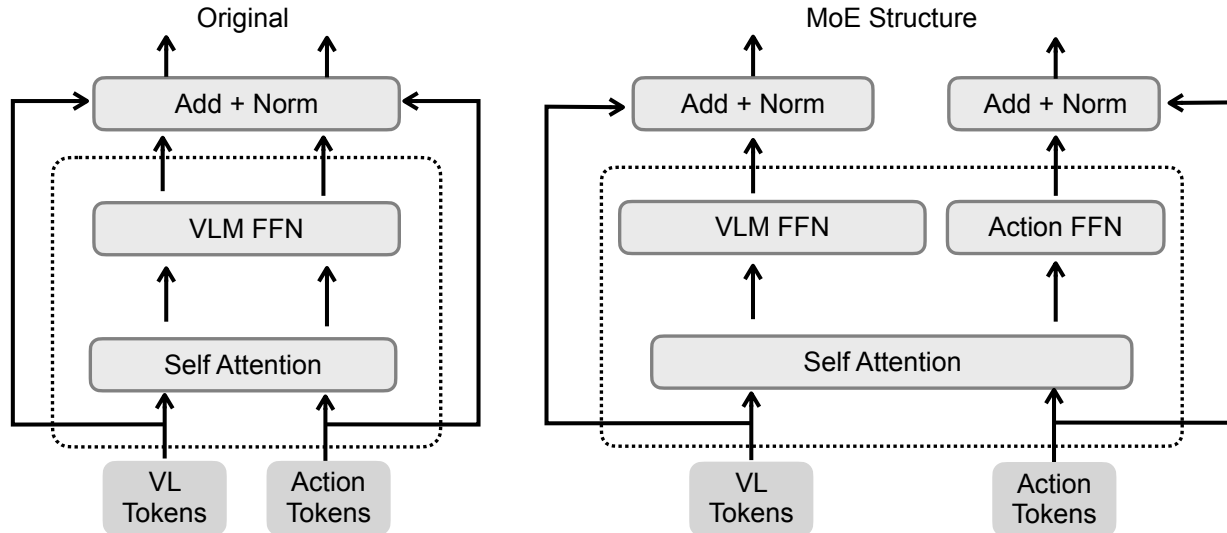
Advising: Huaping Liu, Tao Kong, Hanbo Zhang, Xiao Ma, Bingyi Kang, Di Guo, Xinlong Wang



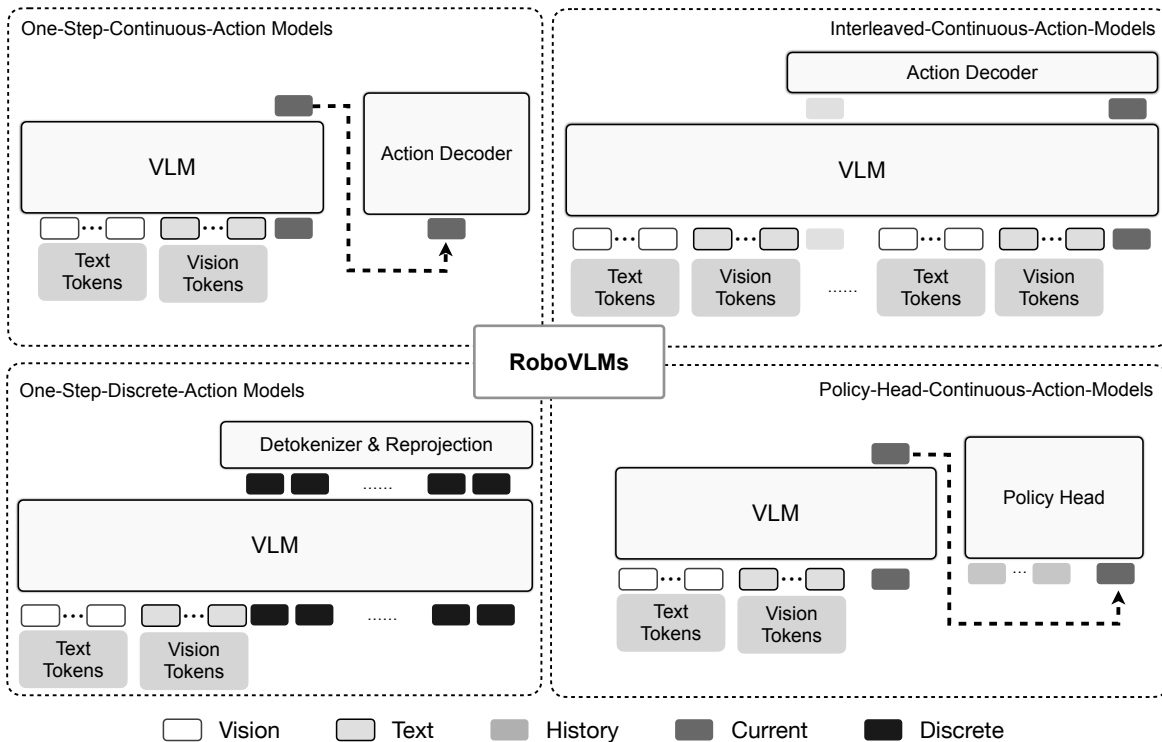
Extended Figure 1: Visualization for rollouts that the best setting VLA built by RoboVLMs emerges the ability of self-correction. For instance, in the Open The Oven task, the robot's first attempt does not reach the oven handle, and it adjusts the end-effector position to re-locate the handle at the second attempt. Note that the training dataset does not contain this kind of data.

Extended Table 1: The essential questions, research questions, and findings of the study.

Essential Questions	Research Questions	Research Findings
<i>Q1</i> : Why VLAs	<i>Q1.1</i> : Are VLAs a proper choice for building generalist robot policies? <i>Q1.2</i> : How does the best VLA built with RoboVLMs perform in real-world scenarios?	<i>A1.1</i> : VLA is a promising path towards generalist robot policies. <i>A1.2</i> : The best setup VLA built with RoboVLMs appears strong effectiveness and robustness in real-world scenarios.
<i>Q2</i> : Which Backbone	<i>Q2</i> : Which type of VLMs are more suitable for constructing VLAs?	<i>A2</i> : Sufficient vision-language pre-trained on large vision-language datasets benefit VLAs
<i>Q3</i> : How to Formulate	<i>Q3.1</i> : How to select the best-performing VLA structure ? <i>Q3.2</i> : How do different formulations affect the generalization and data efficiency for VLAs? <i>Q3.3</i> : How to design appropriate training objective and execution paradigm ? <i>Q3.4</i> : Does Mix-of-Expert structure benefit VLA learning?	<i>A3.1</i> : Continuous action space with policy head to integrate history is the best structure. <i>A3.2</i> : Leveraging policy head for history fusion is the best in terms of generalization and data efficiency. <i>A3.3</i> : Diffusion and MSE training loss are comparable, executing action chunk is efficient and effective. <i>A3.4</i> : Introducing the Mix-of-Expert structure can improve the performance and generalization of VLAs.
<i>Q4</i> : When to Leverage Extra Data	<i>Q4</i> : Which training stage should introduce cross-embodiment datasets?	<i>A4</i> : 1) Extra in-domain data shows beneficial; 2) Post-training further improves high-frequency tasks as well as few-shot performance.

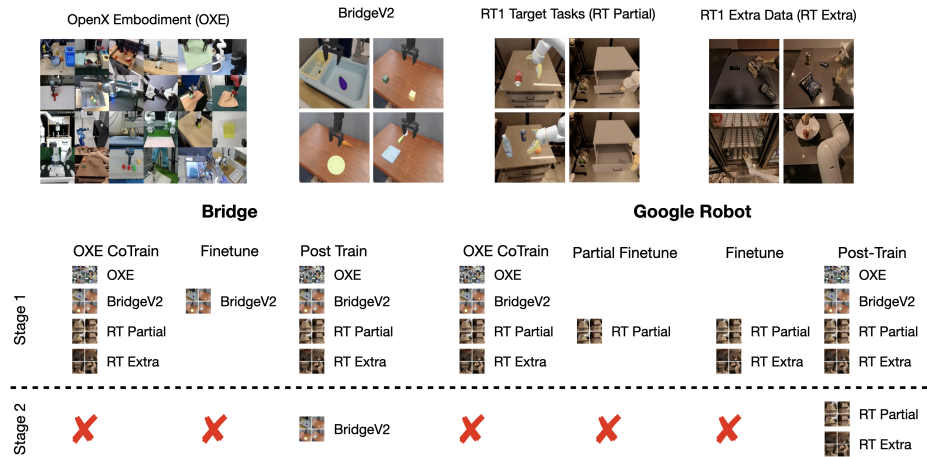


(a) Illustration of Mix-of-Expert structure. In original VLAs, both vision-language tokens and action tokens share the same weights of the original VLM FFN (Feed Forward Network). For the Mix-of-Expert structure, vision-Language tokens and action tokens have separate query, key and value projection layers for self-attention, and have separate feed-forward networks. Action tokens would only interact with vision-language tokens through self-attention. This Mix-of-Expert structure preserves the original parameters and forward process of the VLMs, and is claimed to benefit the generalization for the built VLAs.

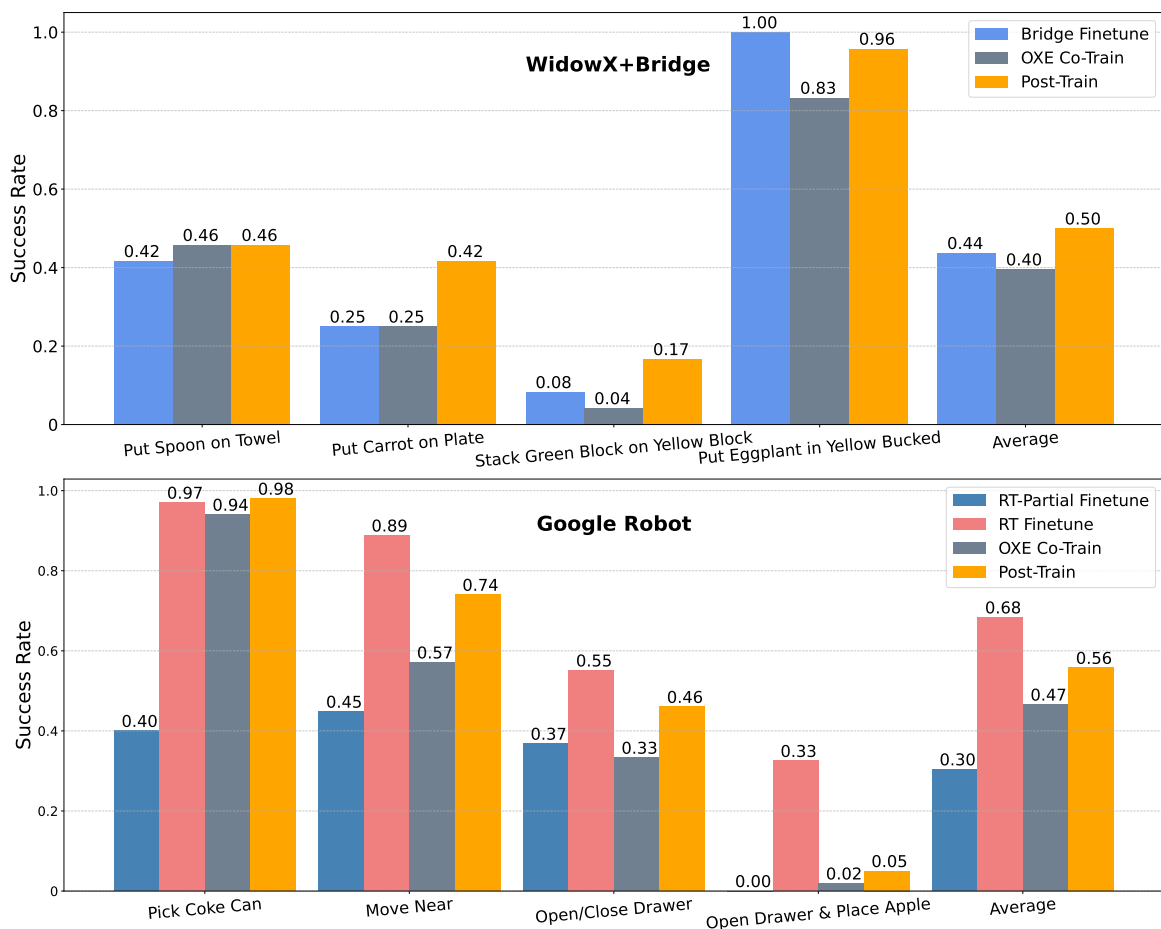


(b) The illustration of considered VLA formulations, including several popular designs. For example, RoboFlamingo [22] is a Policy-Head-Continuous-type VLA, RT-2 [7] and OpenVLA [20] corresponds to the One-Step-Discrete-Action-type VLA. Octo [38] and GR [45] correspond to the Interleaved-Continuous-Action-type VLA with a fixed window size.

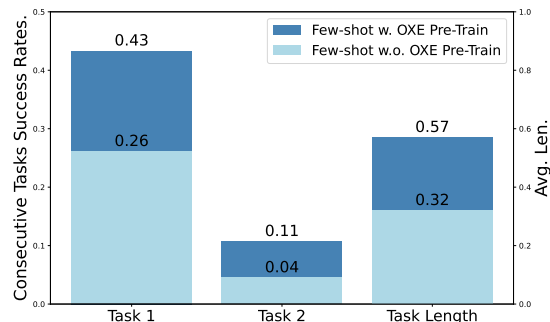
Extended Figure 2: The architectures of MoE and considered VLAs.



Extended Figure 3: Illustration of training configurations for Bridge and Google Robot. The red crosses (X) denote the excluded training stage, and the small icons represent the datasets used, corresponding to those shown above in the figure. Take Bridge Post Train as an example, two stages are employed: Stage 1: Co-training with cross-embodiment data, Bridge V2 dataset, RT1 target dataset, and RT1 extra data. Stage 2: Post-training refinement using only the Bridge V2 dataset.



Extended Figure 4: Ablation studies for cross-embodiment training on **SimpleEnv**. We evaluate four different training recipes. On the *WidowX+Bridge* environments, we test (1) Bridge *Finetune* finetunes the VLA directly on the full Bridge datasets (tested tasks not included); (2) OXE *Co-Train* Co-trains the VLA on OXE dataset [33]; (3) *Post-Train* trains the OXE Co-trained VLA on Bridge datasets. On the *Google Robot* environments, we test (1) *RT-Partial Finetune* finetunes the VLA on tested RT tasks only; (2) *RT Finetune* finetunes the VLA on the full RT dataset (tested tasks included), along with (3) *OXE Co-Train* and (4) *Post-Train* on the tested RT tasks stage.



Extended Figure 5: The effect of cross-embodiment pre-training on OXE datasets for *few-shot learning*.

Extended Table 2: Simulation performances on **CALVIN** benchmark, all models are trained on split ABCD/ABC, and evaluated on split D. KosMos P.H. represents the VLA utilizing KosMos-2 as backbone and policy head as architecture, built with the RoboVLMs framework, and is maximally trained for 5 epochs. We will continue to use the expression of backbone and structure to represent the VLAs built with RoboVLMs in the following paper. Note that KosMos refers to the VLM backbone we utilized, and “P.H.” refers to the policy head formulation.

Method	VLA?	Train	Consecutive tasks success rates					Avg. Len.
			1	2	3	4	5	
MCIL	✗	ABCD	0.373	0.027	0.002	0.000	0.000	0.40
R3M (Frozen)	✗		0.085	0.005	0.001	0.000	0.000	0.10
Voltron (Frozen)	✗		0.101	0.003	0.001	0.000	0.000	0.11
Voltron (Fine-tuned)	✗		0.837	0.566	0.352	0.208	0.115	2.08
RT-1	✗		0.844	0.617	0.438	0.323	0.227	2.45
HULC	✗		0.889	0.733	0.587	0.475	0.383	3.06
GR-1	✓		0.949	0.896	0.844	0.789	0.731	4.21
KosMos P.H. (RoboVLMs)	✓		0.967	0.930	0.899	0.865	0.826	4.49
MCIL	✗	ABC	0.304	0.013	0.002	0.000	0.000	0.31
Voltron (Frozen)	✗		0.026	0.001	0.000	0.000	0.000	0.03
Voltron (Fine-tuned)	✗		0.569	0.272	0.105	0.038	0.014	1.00
RT-1	✗		0.533	0.222	0.094	0.038	0.013	0.90
HULC	✗		0.418	0.165	0.057	0.019	0.011	0.67
GR-1	✓		0.854	0.712	0.596	0.497	0.401	3.06
KosMos P.H. (RoboVLMs)	✓		0.980	0.936	0.854	0.778	0.704	4.25

Extended Table 3: The detailed performance on SimplierEnv.

(a) Simulation performance on **SimplierEnv-WidowX+Bridge** environments. We report both the final success rates (final) along with the sub-task success rates (e.g., Grasp Spoon).

Method	Put Spoon on Towel		Put Carrot on Plate		Stack Green Block on Yellow Block		Put Eggplant in Yellow Basket	
	Grasp Spoon	final	Grasp Carrot	final	Grasp Green Block	final	Grasp Eggplant	final
RT-1-X	0.167	0.000	0.208	0.042	0.083	0.000	0.000	0.000
Octo-Base	0.347	0.125	0.528	0.083	0.319	0.000	0.667	0.431
Octo-Small	0.778	0.472	0.278	0.097	0.403	0.042	0.875	0.569
OpenVLA-7b	0.041	0.000	0.333	0.000	0.125	0.000	0.083	0.041
RoboVLMs (Ours)	0.583	0.458	0.458	0.417	0.375	0.167	0.958	0.958

(b) Simulation performance on **SimplierEnv-Google Robot** environments.

Method	Pick Coke Can				Move Near	Open/Close Drawer			Open Top Drawer and Place Apple
	Horizontal Laying	Vertical Laying	Standing	Average	Average	Open	Close	Average	Average
RT-1 (Converged)	0.960	0.900	0.710	0.857	0.442	0.601	0.861	0.730	0.000
RT-1 (15%)	0.860	0.790	0.480	0.710	0.354	0.463	0.667	0.565	0.000
RT-1-X	0.820	0.330	0.550	0.567	0.317	0.296	0.891	0.597	0.213
RT-2-X	0.740	0.740	0.880	0.787	0.779	0.157	0.343	0.250	0.037
Octo-Base	0.210	0.210	0.090	0.170	0.042	0.009	0.444	0.227	0.000
RT-1 (Begin)	0.050	0.000	0.030	0.027	0.050	0.000	0.278	0.139	0.000
OpenVLA-7b	0.270	0.030	0.190	0.163	0.462	0.194	0.518	0.356	0.000
RoboVLMs (Ours)	1.000	0.910	1.000	0.970	0.888	0.565	0.537	0.551	0.325

(c) Results on WidowX + Bridge setup for cross-embodiment dataset.

Method	Put Spoon on Towel		Put Carrot on Plate		Stack Green Block on Yellow Block		Put Eggplant in Yellow Basket	
	Grasp Spoon	final	Grasp Carrot	final	Grasp Green Block	final	Grasp Eggplant	final
Cross-Emb Pre-Train	0.458	0.458	0.333	0.250	0.458	0.042	0.916	0.833
In-domain Full Finetune	0.625	0.417	0.500	0.250	0.417	0.083	1.000	1.000
Post Train	0.583	0.458	0.458	0.417	0.375	0.167	0.958	0.958

(d) Results on WidowX + Bridge setup for cross-embodiment dataset.

Method	Pick Coke Can				Move Near	Open/Close Drawer			Open Top Drawer and Place Apple
	Horizontal Laying	Vertical Laying	Standing	Average	Average	Open	Close	Average	Average
Cross-Emb Pre-Train	0.940	0.840	0.890	0.890	0.571	0.222	0.444	0.333	0.019
Target Task Finetune	0.420	0.320	0.440	0.400	0.448	0.167	0.567	0.368	0.000
In-domain Full Finetune	1.000	0.910	1.000	0.970	0.888	0.565	0.537	0.551	0.325
Post Train	0.990	0.960	1.000	0.980	0.740	0.250	0.670	0.460	0.050

Extended Table 4: The performance of VLAs implemented with different formulations and training data scales. The results for 0.1x and 1x data are the best-behaved model checkpoints within 5 epochs, and the results for 5x data are the model performance at 1st epoch. We name different implemented VLAs by their VLM backbones and the way of history modeling. Results are reported with models trained maximally within 5 epochs on the ABCD training splits.

VLA Architecture	Data Scale	Consecutive tasks success rates					Avg. Len.
		1	2	3	4	5	
Flamingo P.H. 3B	0.1x	0.120	0.007	0.000	0.000	0.000	0.13
Flamingo P.H. 4B		0.448	0.084	0.014	0.003	0.001	0.55
Flamingo P.H. 9B		0.547	0.190	0.067	0.020	0.003	0.83
KosMos Inter.		0.938	0.701	0.445	0.270	0.140	2.49
KosMos P.H.		0.958	0.684	0.431	0.270	0.176	2.52
Flamingo P.H. 3B	1x	0.964	0.896	0.824	0.740	0.662	4.09
Flamingo P.H. 4B		0.936	0.847	0.750	0.667	0.586	3.79
Flamingo P.H. 9B		0.955	0.879	0.784	0.714	0.634	3.97
KosMos Inter.		0.987	0.915	0.824	0.737	0.660	4.12
KosMos P.H.		0.967	0.930	0.899	0.865	0.826	4.49
Flamingo P.H. 3B	5x	0.971	0.916	0.856	0.794	0.716	4.21
KosMos Inter.		0.989	0.940	0.892	0.842	0.795	4.46
KosMos P.H.		0.968	0.937	0.903	0.872	0.830	4.51

Extended Table 5: The performance of the built VLAs based on VLMs with different image token numbers and VL pre-train data scales. The first three rows are flamingo backbones with encoder-decoder structures, the rest backbones are decoder-only structures. Note that for VLMs with multi-stage training, the data scale refers to the data amount utilized for the final stage of fine-tuning. “UNK” denotes unknown. Results are reported with the model checkpoints trained with 5 epochs on the ABCD training splits, all models are trained with a single side view image for fair comparison. We surprisingly found that both LLaVA and Qwen behave badly without an additional resampler to downsample the number of tokens.

Backbone	#Token	Data Scale	Model Size	Consecutive tasks success rates					Avg. Len.
				1	2	3	4	5	
Flamingo	64	1B+	3B	0.692	0.418	0.241	0.14	0.074	1.57
Flamingo	64	1B+	4B	0.689	0.456	0.281	0.181	0.107	1.71
Flamingo	64	1B+	9B	0.744	0.485	0.298	0.187	0.112	1.83
Qwen-VL	256	350K	9B	0.221	0.062	0.014	0.002	0.000	0.30
MoonDream	576	UNK	3B	0.717	0.473	0.296	0.198	0.127	1.81
Uform	256	10M	1.3B	0.778	0.577	0.407	0.300	0.216	2.28
KosMos	64	90M	2B	0.922	0.807	0.701	0.615	0.549	3.59
Paligemma	256	10B	3B	0.931	0.836	0.752	0.683	0.616	3.82

REFERENCES

- [1] Jean-Baptiste Alayrac, Jeff Donahue, Pauline Luc, Antoine Miech, Iain Barr, Yana Hasson, Karel Lenc, Arthur Mensch, Katherine Millican, Malcolm Reynolds, et al. Flamingo: a visual language model for few-shot learning. *Advances in neural information processing systems*, 35:23716–23736, 2022.
- [2] Jinze Bai, Shuai Bai, Shusheng Yang, Shijie Wang, Sinan Tan, Peng Wang, Junyang Lin, Chang Zhou, and Jingren Zhou. Qwen-vl: A frontier large vision-language model with versatile abilities. *arXiv preprint arXiv:2308.12966*, 2023.
- [3] Lucas Beyer, Andreas Steiner, André Susano Pinto, Alexander Kolesnikov, Xiao Wang, Daniel Salz, Maxim Neumann, Ibrahim Alabdulmohsin, Michael Tschannen, Emanuele Bugliarello, et al. Paligemma: A versatile 3b vlm for transfer. *arXiv preprint arXiv:2407.07726*, 2024.
- [4] Kevin Black, Noah Brown, Danny Driess, Adnan Esmail, Michael Equi, Chelsea Finn, Niccolo Fusai, Lachy Groom, Karol Hausman, Brian Ichter, et al. π_0 : A vision-language-action flow model for general robot control. *arXiv preprint arXiv:2410.24164*, 2024.
- [5] Konstantinos Bousmalis, Giulia Vezzani, Dushyant Rao, Coline Devin, Alex X Lee, Maria Bauza, Todor Davchev, Yuxiang Zhou, Agrim Gupta, Akhil Raju, et al. Robocat: A self-improving foundation agent for robotic manipulation. *arXiv preprint arXiv:2306.11706*, 2023.
- [6] Anthony Brohan, Noah Brown, Justice Carbajal, Yevgen Chebotar, Joseph Dabis, Chelsea Finn, Keerthana Gopalakrishnan, Karol Hausman, Alex Herzog, Jasmine Hsu, et al. Rt-1: Robotics transformer for real-world control at scale. *arXiv preprint arXiv:2212.06817*, 2022.
- [7] Anthony Brohan, Noah Brown, Justice Carbajal, Yevgen Chebotar, Xi Chen, Krzysztof Choromanski, Tianli Ding, Danny Driess, Avinava Dubey, Chelsea Finn, et al. Rt-2: Vision-language-action models transfer web knowledge to robotic control. *arXiv preprint arXiv:2307.15818*, 2023.
- [8] Chi-Lam Cheang, Guangzeng Chen, Ya Jing, Tao Kong, Hang Li, Yifeng Li, Yuxiao Liu, Hongtao Wu, Jiafeng Xu, Yichu Yang, et al. Gr-2: A generative video-language-action model with web-scale knowledge for robot manipulation. *arXiv preprint arXiv:2410.06158*, 2024.
- [9] Cheng Chi, Zhenjia Xu, Siyuan Feng, Eric Cousineau, Yilun Du, Benjamin Burchfiel, Russ Tedrake, and Shuran Song. Diffusion policy: Visuomotor policy learning via action diffusion. *The International Journal of Robotics Research*, page 02783649241273668, 2023.
- [10] Junyoung Chung, Caglar Gulcehre, KyungHyun Cho, and Yoshua Bengio. Empirical evaluation of gated recurrent neural networks on sequence modeling. *arXiv preprint arXiv:1412.3555*, 2014.
- [11] Alexey Dosovitskiy. An image is worth 16x16 words: Transformers for image recognition at scale. *arXiv preprint arXiv:2010.11929*, 2020.
- [12] Chelsea Finn, Pieter Abbeel, and Sergey Levine. Model-agnostic meta-learning for fast adaptation of deep networks. In *International conference on machine learning*, pages 1126–1135. PMLR, 2017.
- [13] Luciano Floridi and Massimo Chiriatti. Gpt-3: Its nature, scope, limits, and consequences. *Minds and Machines*, 30: 681–694, 2020.
- [14] Alex Graves and Alex Graves. Long short-term memory. *Supervised sequence labelling with recurrent neural networks*, pages 37–45, 2012.
- [15] Physical Intelligence, Kevin Black, Noah Brown, James Darpinian, Karan Dhabalia, Danny Driess, Adnan Esmail, Michael Equi, Chelsea Finn, Niccolo Fusai, et al. A vision-language-action model with open-world generalization. *arXiv preprint arXiv:2504.16054*, 2025.
- [16] Andrew Jaegle, Felix Gimeno, Andy Brock, Oriol Vinyals, Andrew Zisserman, and Joao Carreira. Perceiver: General perception with iterative attention. In *International conference on machine learning*, pages 4651–4664. PMLR, 2021.
- [17] Eric Jang, Alex Irpan, Mohi Khansari, Daniel Kappler, Frederik Ebert, Corey Lynch, Sergey Levine, and Chelsea Finn. Bc-z: Zero-shot task generalization with robotic imitation learning, 2022.
- [18] Yunfan Jiang, Agrim Gupta, Zichen Zhang, Guanzhi Wang, Yongqiang Dou, Yanjun Chen, Li Fei-Fei, Anima Anandkumar, Yuke Zhu, and Linxi Fan. Vima: General robot manipulation with multimodal prompts. *arXiv preprint arXiv:2210.03094*, 2022.
- [19] Tsung-Wei Ke, Nikolaos Gkanatsios, and Katerina Fragkiadaki. 3d diffuser actor: Policy diffusion with 3d scene representations. *arXiv preprint arXiv:2402.10885*, 2024.
- [20] Moo Jin Kim, Karl Pertsch, Siddharth Karamcheti, Ted Xiao, Ashwin Balakrishna, Suraj Nair, Rafael Rafailov, Ethan Foster, Grace Lam, Pannag Sanketi, et al. Openvla: An open-source vision-language-action model. *arXiv preprint arXiv:2406.09246*, 2024.
- [21] Peiyan Li, Hongtao Wu, Yan Huang, Chilam Cheang, Liang Wang, and Tao Kong. Gr-mg: Leveraging partially annotated data via multi-modal goal conditioned policy. *arXiv preprint arXiv:2408.14368*, 2024.
- [22] Xinghang Li, Minghuan Liu, Hanbo Zhang, Cunjun Yu, Jie Xu, Hongtao Wu, Chilam Cheang, Ya Jing, Weinan Zhang, Huaping Liu, et al. Vision-language foundation models as effective robot imitators. *arXiv preprint arXiv:2311.01378*, 2023.

- [23] Xuanlin Li, Kyle Hsu, Jiayuan Gu, Karl Pertsch, Oier Mees, Homer Rich Walke, Chuyuan Fu, Ishikaa Lunawat, Isabel Sieh, Sean Kirmani, et al. Evaluating real-world robot manipulation policies in simulation. [arXiv preprint arXiv:2405.05941](#), 2024.
- [24] Yaron Lipman, Ricky TQ Chen, Heli Ben-Hamu, Maximilian Nickel, and Matt Le. Flow matching for generative modeling. [arXiv preprint arXiv:2210.02747](#), 2022.
- [25] Fanfan Liu, Feng Yan, Liming Zheng, Chengjian Feng, Yiyang Huang, and Lin Ma. Robouniview: Visual-language model with unified view representation for robotic manipulation. [arXiv preprint arXiv:2406.18977](#), 2024.
- [26] Haotian Liu, Chunyuan Li, Qingyang Wu, and Yong Jae Lee. Visual instruction tuning. *Advances in neural information processing systems*, 36, 2024.
- [27] Huaping Liu, Di Guo, and Angelo Cangelosi. Embodied intelligence: A synergy of morphology, action, perception and learning. *ACM Computing Surveys*, 57(7):1–36, 2025.
- [28] Jiaming Liu, Mengzhen Liu, Zhenyu Wang, Lily Lee, Kaichen Zhou, Pengju An, Senqiao Yang, Renrui Zhang, Yandong Guo, and Shanghang Zhang. Robomamba: Multimodal state space model for efficient robot reasoning and manipulation. [arXiv preprint arXiv:2406.04339](#), 2024.
- [29] Larry R Medsker, Lakhmi Jain, et al. Recurrent neural networks. *Design and Applications*, 5(64-67):2, 2001.
- [30] Oier Mees, Lukas Hermann, Erick Rosete-Beas, and Wolfram Burgard. Calvin: A benchmark for language-conditioned policy learning for long-horizon robot manipulation tasks. *IEEE Robotics and Automation Letters*, 7(3):7327–7334, 2022.
- [31] Arsha Nagrani, Shan Yang, Anurag Arnab, Aren Jansen, Cordelia Schmid, and Chen Sun. Attention bottlenecks for multimodal fusion. *Advances in neural information processing systems*, 34:14200–14213, 2021.
- [32] Suraj Nair, Aravind Rajeswaran, Vikash Kumar, Chelsea Finn, and Abhinav Gupta. R3m: A universal visual representation for robot manipulation. [arXiv preprint arXiv:2203.12601](#), 2022.
- [33] Abby O’Neill, Abdul Rehman, Abhinav Gupta, Abhiram Maddukuri, Abhishek Gupta, Abhishek Padalkar, Abraham Lee, Acorn Pooley, Agrim Gupta, Ajay Mandlekar, et al. Open x-embodiment: Robotic learning datasets and rt-x models. [arXiv preprint arXiv:2310.08864](#), 2023.
- [34] Zhiliang Peng, Wenhui Wang, Li Dong, Yaru Hao, Shaohan Huang, Shuming Ma, and Furu Wei. Kosmos-2: Grounding multimodal large language models to the world. [arXiv preprint arXiv:2306.14824](#), 2023.
- [35] Ilija Radosavovic, Tete Xiao, Stephen James, Pieter Abbeel, Jitendra Malik, and Trevor Darrell. Real-world robot learning with masked visual pre-training, 2023.
- [36] Scott Reed, Konrad Zolna, Emilio Parisotto, Sergio Gomez Colmenarejo, Alexander Novikov, Gabriel Barth-Maron, Mai Gimenez, Yury Sulsky, Jackie Kay, Jost Tobias Springenberg, et al. A generalist agent. [arXiv preprint arXiv:2205.06175](#), 2022.
- [37] Noam Shazeer, Azalia Mirhoseini, Krzysztof Maziarz, Andy Davis, Quoc Le, Geoffrey Hinton, and Jeff Dean. Outrageously large neural networks: The sparsely-gated mixture-of-experts layer. *International Conference on Learning Representations*, 2017.
- [38] Octo Model Team, Dibya Ghosh, Homer Walke, Karl Pertsch, Kevin Black, Oier Mees, Sudeep Dasari, Joey Hejna, Tobias Kreiman, Charles Xu, et al. Octo: An open-source generalist robot policy. [arXiv preprint arXiv:2405.12213](#), 2024.
- [39] Marcel Torne, Anthony Simeonov, Zechu Li, April Chan, Tao Chen, Abhishek Gupta, and Pulkit Agrawal. Reconciling reality through simulation: A real-to-sim-to-real approach for robust manipulation. [arXiv preprint arXiv:2403.03949](#), 2024.
- [40] Unum-cloud. Uform: Pocket-sized multimodal ai for content understanding and generation, 2024. URL <https://huggingface.co/unum-cloud/uform-gen2-qwen-500m>.
- [41] A Vaswani. Attention is all you need. *Advances in Neural Information Processing Systems*, 2017.
- [42] Vikhyat. Moondream, tiny vision language model, 2024. URL <https://github.com/vikhyat/moondream>.
- [43] Homer Walke, Kevin Black, Abraham Lee, Moo Jin Kim, Max Du, Chongyi Zheng, Tony Zhao, Philippe Hansen-Estruch, Quan Vuong, Andre He, Vivek Myers, Kuan Fang, Chelsea Finn, and Sergey Levine. Bridgedata v2: A dataset for robot learning at scale, 2023.
- [44] Peng Wang, An Yang, Rui Men, Junyang Lin, Shuai Bai, Zhikang Li, Jianxin Ma, Chang Zhou, Jingren Zhou, and Hongxia Yang. Ofa: Unifying architectures, tasks, and modalities through a simple sequence-to-sequence learning framework, 2022.
- [45] Hongtao Wu, Ya Jing, Chilam Cheang, Guangzeng Chen, Jiafeng Xu, Xinghang Li, Minghuan Liu, Hang Li, and Tao Kong. Unleashing large-scale video generative pre-training for visual robot manipulation. [arXiv preprint arXiv:2312.13139](#), 2023.
- [46] Hu Xu, Gargi Ghosh, Po-Yao Huang, Prahal Arora, Masoumeh Aminzadeh, Christoph Feichtenhofer, Florian Metzger, and Luke Zettlemoyer. Vlm: Task-agnostic video-language model pre-training for video understanding. [arXiv preprint arXiv:2105.09996](#), 2021.
- [47] Zhengyuan Yang, Linjie Li, Kevin Lin, Jianfeng Wang, Chung-Ching Lin, Zicheng Liu, and Lijuan Wang. The dawn of Imms: Preliminary explorations with gpt-4v (ision). [arXiv preprint arXiv:2309.17421](#), 9(1):1, 2023.
- [48] Seonghyeon Ye, Joel Jang, Byeongguk Jeon, Sejune Joo, Jianwei Yang, Baolin Peng, Ajay Mandlekar, Reuben Tan, Yu-Wei Chao, Bill Yuchen Lin, et al. Latent action pretraining from videos. [arXiv preprint arXiv:2410.11758](#), 2024.
- [49] Yang Yue, Yulin Wang, Bingyi Kang, Yizeng Han, Shenzhi Wang, Shiji Song, Jiashi Feng, and Gao Huang. Deer-vla: Dynamic inference of multimodal large language models for efficient robot execution. [arXiv preprint arXiv:2411.02359](#),

2024.

- [50] Michał Zawalski, William Chen, Karl Pertsch, Oier Mees, Chelsea Finn, and Sergey Levine. Robotic control via embodied chain-of-thought reasoning. [arXiv preprint arXiv:2407.08693](#), 2024.
- [51] Tony Z Zhao, Vikash Kumar, Sergey Levine, and Chelsea Finn. Learning fine-grained bimanual manipulation with low-cost hardware. [arXiv preprint arXiv:2304.13705](#), 2023.
- [52] Wenshuai Zhao, Jorge Peña Queraltá, and Tomi Westerlund. Sim-to-real transfer in deep reinforcement learning for robotics: a survey, 2020.
- [53] Haoyu Zhen, Xiaowen Qiu, Peihao Chen, Jincheng Yang, Xin Yan, Yilun Du, Yining Hong, and Chuang Gan. 3d-vla: A 3d vision-language-action generative world model. [arXiv preprint arXiv:2403.09631](#), 2024.
- [54] Zhongyi Zhou, Yichen Zhu, Junjie Wen, Chaomin Shen, and Yi Xu. Vision-language-action model with open-world embodied reasoning from pretrained knowledge. [arXiv preprint arXiv:2505.21906](#), 2025.

APPENDIX A DISCUSSION

This empirical study mainly focuses on what matters in building Visual-Language-Action models (VLAs). We raise four essential questions for building a VLA: **Why** do we need VLAs instead of other generalist policies, and by outperforming the existing methods by a large margin, we illustrate the necessity of studying VLAs. For the next step, we describe the key components for building a VLM-based VLA: **Which** kind of VLM backbone to utilize, **How** to train the model to generate action, and **When** should we add cross-embodiment data into training stages. To answer these questions, we built a unified framework for a fair comparison of VLAs and designed a series of bottom-up systematic experiments. To answer these questions, we conduct extensive experiments across three simulators and more than 240 rollouts within 20 tasks in real-world scenarios, and we can conclude from the experiments that: For the **Why** question, VLAs could achieve high performance and generalization, and is a promising path to generalist robotics policy; For the **Which** problem, we find that VLMs with sufficient vision-language pre-training over large scale vision-language datasets is suitable for constructing VLAs. For the **How** problem, we can investigate the performance, generalization, and data efficiency of different VLA structures, and find that integrating history observations is essential for VLAs, and policy head is a more effective and efficient history aggregating method compared with interleaved; For the **When** problem, we compare three training recipes with cross-embodiment integrated at different stages, and conclude that extra in-domain data shows beneficial, and large-scale cross-embodiment pre-training further improves overall as well as few-shot performance. As a byproduct of answers to the raised questions, we built an easy-to-use framework for easily integrating arbitrary VLMs and turning them into VLAs, named **RoboVLMs**.

Under investigated observations. During our experiments, we found that VLAs built upon Qwen-VL and LLaVA, the performance is surprisingly low, compared with their original performance on vision-language tasks. After adding a perceiver resampler after the vision encoder, we found that the VLAs based on Qwen-VL and LLaVA could obtain great performance gains and reach reasonable performance. We hypothesize that the performance gain is related to the image resolution and the number of vision tokens in the input token sequence.

Limitations. Although we make every effort to investigate the key challenges in building Vision-Language Agents (VLAs), this work remains preliminary and has several limitations at the current stage. (1) The action tokenization, policy head, and corresponding training objectives are not fully explored in this work. For example, techniques like VQ-VAE, VQGAN, and FAST action tokenizer remain under-explored in the context of VLAs. (2) The set of VLM backbones considered in this study is limited and can be actively expanded. (3) Deploying such large models for real-time robotic control remains a significant challenge.

Future works. For future work, we envision several potential directions for advancing generalist robot policies. Beyond semantic generalization, an ideal generalist robot policy should be capable of handling long-horizon, complex task instructions (e.g., make breakfast), reasoning through executable actions step by step, and generating meaningful physical interactions with its environment. In our future work, we aim to explore the key elements required to develop policies with these advanced capabilities.

We have open-sourced our codebase with detailed guidelines, model weights of the strongest VLAs built by RoboVLMs, along with the real-world dataset used in our experiments. We anticipate that our research will bolster the community and expedite progress in the realms of vision-language learning and foundational models for robotics.

APPENDIX B IMPLEMENTATION DETAILS

a) Hyper-parameters and Training Details.: With different formulations, the best setting of hyperparameters like batch size, weight decay, and learning rate could be varied. Although OpenVLA suggests utilizing the same hyperparameters as in the VLM pretrain phase, we find that a varied setting of the hyperparameters could improve the performance.

The hyperparameters for fine-tuning VLAs are mainly derived from the VLMs training setups, for example, we select the weight decay from $[0, 1e - 1]$, and the learning rate as one of $[1e - 4, 5e - 5, 2e - 5, 1e - 5]$. We conduct a grid search and select the one with the best performance. We set the global batch size as 128 and the warmup ratio is 0.25 epoch (5K steps for OpenX Embodiment pre-train). All models included in this paper are trained on a cluster of 4 x 8 A100-80G GPUs.

b) Checkpoint selection.: We find out that, normally, the performance of robot policies does not fully depend on offline evaluation metrics, such as the validation loss, due to the compounding error in long-horizon rollouts. Therefore, it is challenging to select the best checkpoint during training. For fair comparisons, we train all VLAs for a fixed number of epochs or timesteps. Concretely, on CALVIN, we train each model for 5 epochs with a batch size of 128 truncated trajectories and report the performance of the final model. For SimplerEnv, we train the model for 100K iterations with a batch size of 512 truncated trajectories and report the best-performing model with a 10K-iteration training interval. In real-world experiments, we train the model for 5 epochs with a batch size of 512 truncated trajectories, and we only report the performance of the last model.

Supplementary Table 1: Hyper Parameters setup for different experiments. ‘‘EP’’ denotes the epoch. ‘‘Iters’’ represents iterations.

Experiment Name	Backbone	Window Size	Chunk Size	Input View	Batch Size	Warmup	Scheduler	Optimizer	Learning Rate	Total Epochs/Iters
CALVIN Perform (Extended Table. 2)	KosMos-2	16	10	Side+Wrist	128	0.25 Ep	Constant	AdamW	1e-4	5 Ep
SimplerEnv Training Recipe (Supplementary Fig. 1, Extended Fig.4)	PaliGemma (Co-Train)	1	10	Side	1024	500 Iters	Constant	AdamW	2e-5	20K Iters
	PaliGemma (Post-Train & Finetune)	1	10	Side	128	0.25 Ep	Constant	AdamW	5e-5	5 Ep
CALVIN VL Pre-train (Fig. 4b)	Flamingo & KosMos-2	16	10	Side+Wrist	128	0.25 Ep	Constant	AdamW	1e-4	5 Ep
Real Perform (Fig. 4d)	KosMos-2	8	10	Side+Wrist	128	0.25 Ep	Constant	AdamW	1e-4	5 Ep
VLA Structure (Table. I)	LLaVA	8	10	Side+Wrist	128	0.25 Ep	Constant	AdamW	2e-5	5 Ep
	Flamingo & KosMos-2 & PaliGemma	16	10	Side+Wrist	128	0.25 Ep	Constant	AdamW	1e-4	5 Ep
CALVIN Generalization (Fig. 4c)	All	16	10	Side+Wrist	128	0.25 Ep	Constant	AdamW	1e-4	5 Ep
CALVIN Data Efficiency (Extended Table. 4)	All	16	10	Side+Wrist	128	0.25 Ep	Constant	AdamW	1e-4	5 Ep
CALVIN Backbone (Extended Table. 5)	All	8	10	Side	128	0.25 Ep	Constant	AdamW	2e-5	5 Ep
CALVIN Training Objective (Table. IIa)	All	1	10	Side+Wrist	128	0.25 Ep	Constant	AdamW	2e-5	5 Ep
CALVIN MoE (Table. IIb)	All	1	10	Side+Wrist	128	0.25 Ep	Constant	AdamW	2e-5	5 Ep
CALVIN few-shot (Extended Fig. 5)	All	16	10	Side	128	0 Iter	Constant	AdamW	2e-5	5K Iters

APPENDIX C BENCHMARK DETAILS

CALVIN is a simulated benchmark for multi-task table-top manipulation. It provides 24k human-teleoperated demonstrations annotated with language instruction. Each trajectory is less than 64-time steps, which includes 34 pre-defined basic skills: rotate blue block right, move slider right, lift red block slider, place slider, turn off light bulb, turn off led light, push in drawer, lift blue block drawer, close drawer, lift pink block slider, lift pink block table, move slider left, open drawer, turn on light bulb, rotate blue block left, push blue block left, rotate red block right, turn on led light, push pink block right, push red block left, lift blue block table, place in drawer, rotate red block left, push pink block left, lift stacked blocks, lift blue block slider, push red block right. The dataset contains four splits as scene A, B, C, and D. We train and test VLAs on different training/test splits to fully analyze the capabilities, data and training efficiencies. During evaluation, the robot is required to complete a set of 5 consecutive tasks. The metrics are the success rates of finishing these sequential tasks and the average length of completed tasks. All evaluations are implemented on D split, with 1000 rollouts and 5 consecutive sub-tasks for each rollout.

SimplerEnv are designed as a suite of real-to-sim environments, which enables evaluating robotic policies in simulation as efficient, scalable, and informative alternative to real-world evaluation. SimplerEnv created a comparable arena for benchmarking robotics policies on private real-world setups as Google and BridgeData V2.

We adopt the following tasks in the Google Robot setting:

- **pick coke can.** The task assigned to the robot is to pick up an empty Coke can from the table and lift it. Under the standard configuration, the environment is kept free of any distracting elements. The Coke can is arranged in three distinct positions: lying flat horizontally, lying flat vertically, and standing upright. For each of these positions, the can is placed at 25 specific grid points within a defined rectangular area on the table. This setup results in 25 experiments per position, totaling 75 trials across all orientations.
- **move {obj1} near {obj2}.** In the experiment, a set of three objects was arranged on the table in a triangular formation. For each trial, one object was assigned the role of the source, another was designated as the target, and the third served as a distractor. This setup resulted in six distinct trials for each triplet and triangular configuration. From a total of eight objects—blue plastic bottle, Pepsi can, orange, 7up can, apple, sponge, Coke can, and Redbull can—five triplets were randomly selected. Additionally, two triangular patterns, upright and inverted, were employed. This design produced a total of 60 trials.
- **(open/close) (top / middle/bottom) drawer.** In this setup, the robot is placed facing a cabinet equipped with three drawers and tasked with opening or closing a specific drawer. This experiment evaluates the robot’s capability to handle articulated objects. The robot is positioned at nine distinct locations on a predefined grid within a rectangular area on the floor. With three drawers and two possible actions (opening or closing), the setup results in a total of 54 trials.
- **open top drawer; place apple into top drawer.** In this experiment, the robot is tasked with opening the top drawer and transferring an apple from the surface of the cabinet into the drawer. This setup evaluates the robot’s ability to execute tasks that require multiple sequential actions. The robot is positioned in three distinct locations on the floor, while the apple is placed at nine specific grid points on the cabinet surface, resulting in a total of 27 trials. At the start, the robot operates under the instruction to open the top drawer. Once the robot either signals task completion with a "terminate" token or reaches the midpoint of the allotted time, the instruction transitions to directing the robot to place the apple into the drawer.

For the WidowX + Bridge setting, we test the following tasks:

- **put the spoon on the towel.** In this setup, the spoon is positioned at one corner of a square on the tabletop, with the towel placed at a different corner. The square has sides measuring 15 cm in length. The orientation of the spoon

alternates between horizontal and vertical, requiring the robot to adjust the orientation of its gripper accordingly. This configuration results in a total of 24 trials.

- **put carrot on plate.** This setup is similar to put the spoon on the towel, but the spoon is replaced with a carrot and the towel is substituted with a plate.
- **stack the green block on the yellow block.** In this experiment, a green block is positioned at one corner of a square on the tabletop, while a yellow block is placed at a different corner. Both blocks measure 3 cm in size. Two square configurations with 10 cm and 20 cm side lengths are used. This setup results in a total of 24 trials.
- **put eggplant into yellow basket.** An eggplant is positioned randomly within the right basin of a sink, while a yellow basket is placed in the left basin. The eggplant's placement varies in both location and orientation but is carefully arranged to remain easily graspable, avoiding proximity to the sink's edges. A total of 24 trials are conducted under this setup.

APPENDIX D
DETAILED PERFORMANCE ON CALVIN

Supplementary Table 2: Generalization and data efficiency of VLAs with or without vision-language pre-train on different settings of the CALVIN benchmark. "Inter." denotes interleaved modeling. "P.H." denotes policy head. "No VL" suggests models without VL pre-training. "5x" represents training with 5x re-generated training data. The results for 5x data are the model performance at 1 epoch, and the best-behaved model checkpoints within 5 epochs for the others.

Architecture	Train	Consecutive tasks success rates					Avg. Len.
		1	2	3	4	5	
KosMos Inter. No VL		0.692	0.382	0.189	0.085	0.036	1.38
KosMos Inter.		0.987	0.915	0.824	0.737	0.660	4.12
KosMos P.H. No VL	ABCD	0.815	0.626	0.473	0.349	0.245	2.51
KosMos P.H.		0.967	0.930	0.899	0.865	0.826	4.49
Flamingo P.H. 9B No VL		0.733	0.444	0.270	0.161	0.077	1.69
Flamingo P.H. 9B		0.955	0.879	0.784	0.714	0.634	3.97
KosMos Inter. No VL	5x ABCD	0.833	0.588	0.421	0.297	0.209	2.35
KosMos Inter.		0.989	0.940	0.892	0.842	0.795	4.46
KosMos P.H. No VL		0.893	0.755	0.644	0.564	0.462	3.32
KosMos P.H.		0.968	0.937	0.903	0.872	0.830	4.51
KosMos Inter. No VL	ABC	0.432	0.162	0.044	0.007	0.002	0.65
KosMos Inter.		0.824	0.684	0.524	0.376	0.296	2.70
KosMos P.H. No VL		0.389	0.121	0.038	0.008	0.001	0.56
KosMos P.H.		0.980	0.936	0.854	0.778	0.704	4.25

APPENDIX E
DIVERSE BACKBONE

Supplementary Table 3: Sub-task level success rates by tasks in CALVIN under different VLM backbones. All models trained with 5 epochs on CALVIN ABCD training splits.

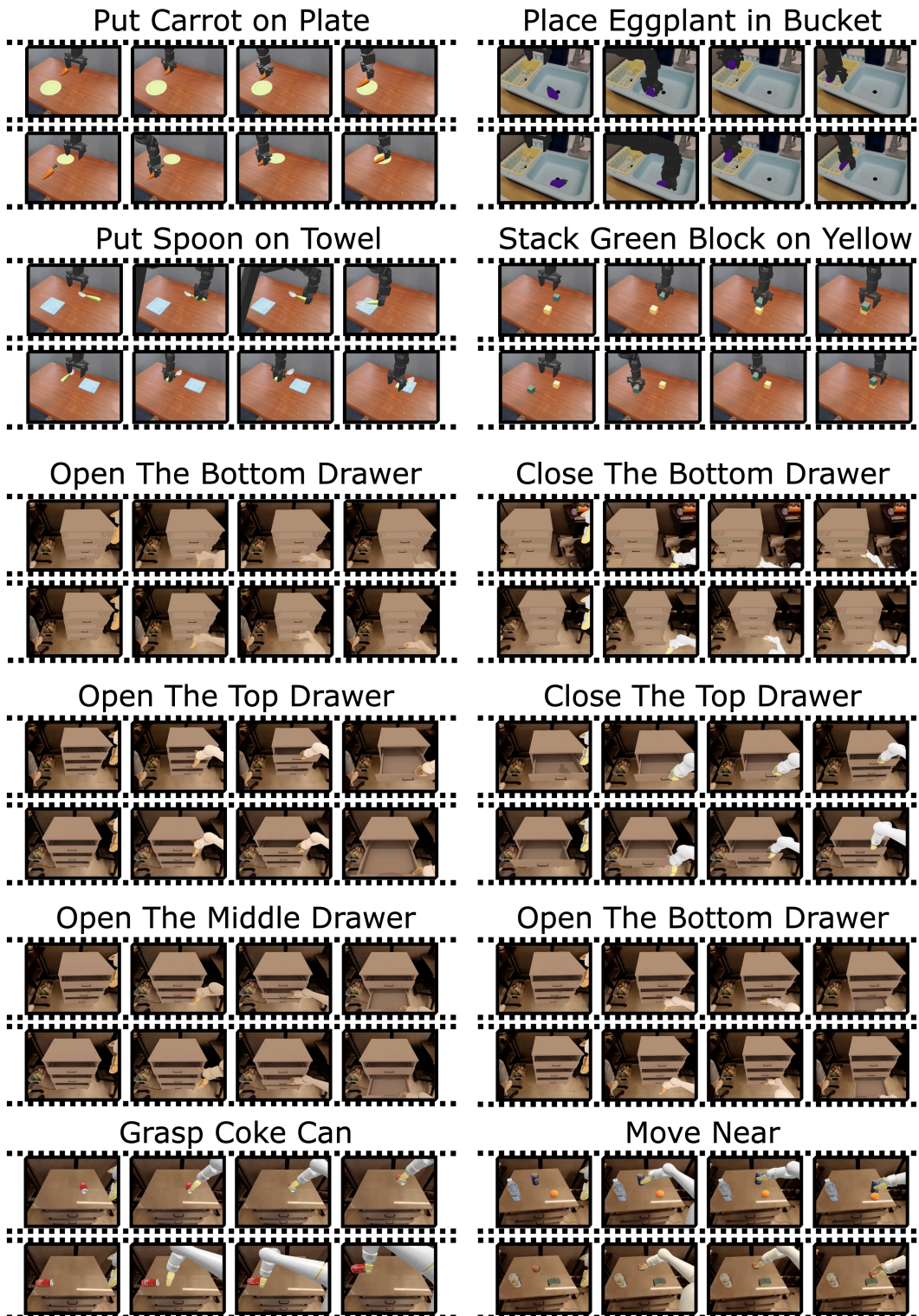
Task Name	Flamingo- 3B	Flamingo- 4B	Flamingo- 9B	KosMos	MoonDrean	Paligemma	Qwen	Uform
rotate blue block right	0.222	0.300	0.322	0.493	0.234	0.816	0.057	0.689
move slider right	0.736	0.989	0.805	0.987	0.988	1.000	0.442	1.000
lift red block slider	0.681	0.620	0.301	0.856	0.500	0.975	0.051	0.387
place in slider	0.683	0.813	0.765	0.874	0.361	0.957	0.308	0.490
turn off lightbulb	0.935	0.920	0.857	0.927	0.988	0.992	0.051	0.907
turn off led	0.990	0.925	0.966	0.970	0.990	0.987	0.793	0.754
push into drawer	0.422	0.318	0.296	0.705	0.688	0.814	0.000	0.743
lift blue block drawer	1.000	1.000	0.250	0.917	0.833	1.000	–	0.917
close drawer	0.118	1.00	0.990	0.986	0.991	1.000	0.160	0.950
lift pink block slider	0.754	0.633	0.471	0.861	0.444	0.945	0.059	0.703
lift pink block table	0.708	0.541	0.630	0.543	0.544	0.936	0.229	0.892
move slider left	0.952	0.952	0.961	0.970	1.000	1.000	0.787	0.994
open drawer	0.986	0.796	0.983	0.980	1.000	1.000	0.231	0.992
turn on lightbulb	0.737	0.225	0.561	0.949	0.990	1.000	0.170	0.775
rotate blue block left	0.358	0.588	0.596	0.636	0.500	0.955	0.000	0.964
push blue block left	0.554	0.509	0.696	0.677	0.424	0.727	0.000	0.661
rotate red block right	0.267	0.317	0.355	0.591	0.444	0.853	0.162	0.610
turn on led	0.962	0.864	0.902	0.985	0.973	0.970	0.562	0.526
push pink block right	0.365	0.574	0.538	0.627	0.271	0.559	0.027	0.412
push red block left	0.383	0.542	0.727	0.562	0.338	0.653	0.043	0.435
lift blue block table	0.470	0.474	0.564	0.611	0.691	0.955	0.111	0.889
place in drawer	0.969	0.932	0.928	0.971	0.958	0.994	0.750	0.931
rotate red block left	0.469	0.562	0.588	0.677	0.327	0.937	0.000	0.978
push pink block left	0.661	0.672	0.697	0.747	0.338	0.857	0.000	0.554
stack block	0.130	0.029	0.070	0.569	0.448	0.646	0.000	0.495
lift blue block slider	0.458	0.405	0.282	0.769	0.867	0.953	0.211	0.367
push red block right	0.233	0.561	0.557	0.457	0.194	0.414	0.103	0.350
lift red block table	0.629	0.608	0.554	0.606	0.640	0.967	0.091	0.835
lift pink block drawer	0.800	0.667	0.333	0.778	0.667	0.929	–	0.400
rotate pink block right	0.182	0.358	0.377	0.478	0.462	0.620	0.179	0.431
unstack block	1.000	0.500	1.000	0.946	0.950	0.935	–	0.880
rotate pink block left	0.578	0.442	0.479	0.698	0.146	0.964	0.034	1.000
push blue block right	0.091	0.421	0.320	0.400	0.066	0.324	0.000	0.500
lift red block drawer	0.400	0.625	0.800	0.769	0.667	1.000	–	0.556

APPENDIX F
DIVERSE PH

Supplementary Table 4: Sub-task level success rates by tasks in CALVIN under different training splits and VLM backbones. All models are trained with maximal 5 epochs.

Task Name	flamingo-3b-abc	flamingo-3b-abcd	flamingo-4b-abcd	flamingo-9b-abc	flamingo-9b-abcd	kosmos-abc	kosmos-abcd
rotate blue block right	0.831	0.893	0.770	0.722	0.882	0.960	0.974
move slider right	0.163	0.993	0.992	0.471	0.996	1.000	1.000
lift red block slider	0.642	0.970	0.858	0.610	0.927	0.906	0.993
place in slider	0.739	0.828	0.911	0.654	0.910	0.744	0.960
turn off lightbulb	0.852	1.000	0.956	0.135	0.964	1.000	1.000
turn off led	0.835	1.000	0.994	0.765	0.981	0.970	1.000
push into drawer	0.656	0.821	0.770	0.688	0.703	0.805	0.849
lift blue block drawer	0.818	0.950	1.000	0.800	0.737	0.944	1.000
close drawer	1.000	1.000	1.000	0.978	0.995	1.000	1.000
lift pink block slider	0.674	0.971	0.862	0.733	0.918	0.925	0.993
lift pink block table	0.871	0.851	0.892	0.872	0.899	0.913	0.961
move slider left	0.517	0.996	1.000	0.798	0.996	0.992	1.000
open drawer	1.000	0.997	0.982	0.991	0.997	1.000	1.000
turn on lightbulb	0.922	0.994	0.988	0.241	0.988	0.989	1.000
rotate blue block left	0.915	0.939	0.925	0.755	0.848	0.985	1.000
push blue block left	0.909	0.955	0.836	0.736	0.909	0.914	0.826
rotate red block right	0.893	0.972	0.905	0.727	0.959	1.000	0.973
turn on led	0.956	0.988	0.976	0.777	0.994	0.977	0.995
push pink block right	0.706	0.754	0.651	0.652	0.750	0.708	0.779
push red block left	0.983	0.920	0.949	0.911	0.908	0.910	0.848
lift blue block table	0.936	0.956	0.927	0.876	0.931	0.995	0.995
place in drawer	1.000	0.989	0.975	0.969	0.976	1.000	1.000
rotate red block left	0.942	0.908	0.953	0.961	0.952	1.000	1.000
push pink block left	0.889	0.920	0.973	0.959	0.933	0.959	0.883
stack block	0.489	0.641	0.595	0.588	0.604	0.801	0.908
lift blue block slider	0.607	0.963	0.826	0.595	0.869	0.835	0.978
push red block right	0.825	0.732	0.451	0.764	0.653	0.871	0.681
lift red block table	0.891	0.939	0.975	0.958	0.989	0.989	0.984
lift pink block drawer	0.444	0.800	0.714	0.333	0.923	0.846	0.857
rotate pink block right	0.768	0.896	0.794	0.787	0.789	0.985	0.986
unstack block	0.880	0.982	0.980	0.909	0.979	0.985	1.000
rotate pink block left	0.974	0.839	0.818	0.947	0.927	1.000	0.965
push blue block right	0.620	0.597	0.478	0.511	0.594	0.870	0.657
lift red block drawer	0.714	1.000	1.000	0.833	0.933	0.950	1.000

APPENDIX G
 ROLLOUT EXAMPLES IN SIMPLERENV

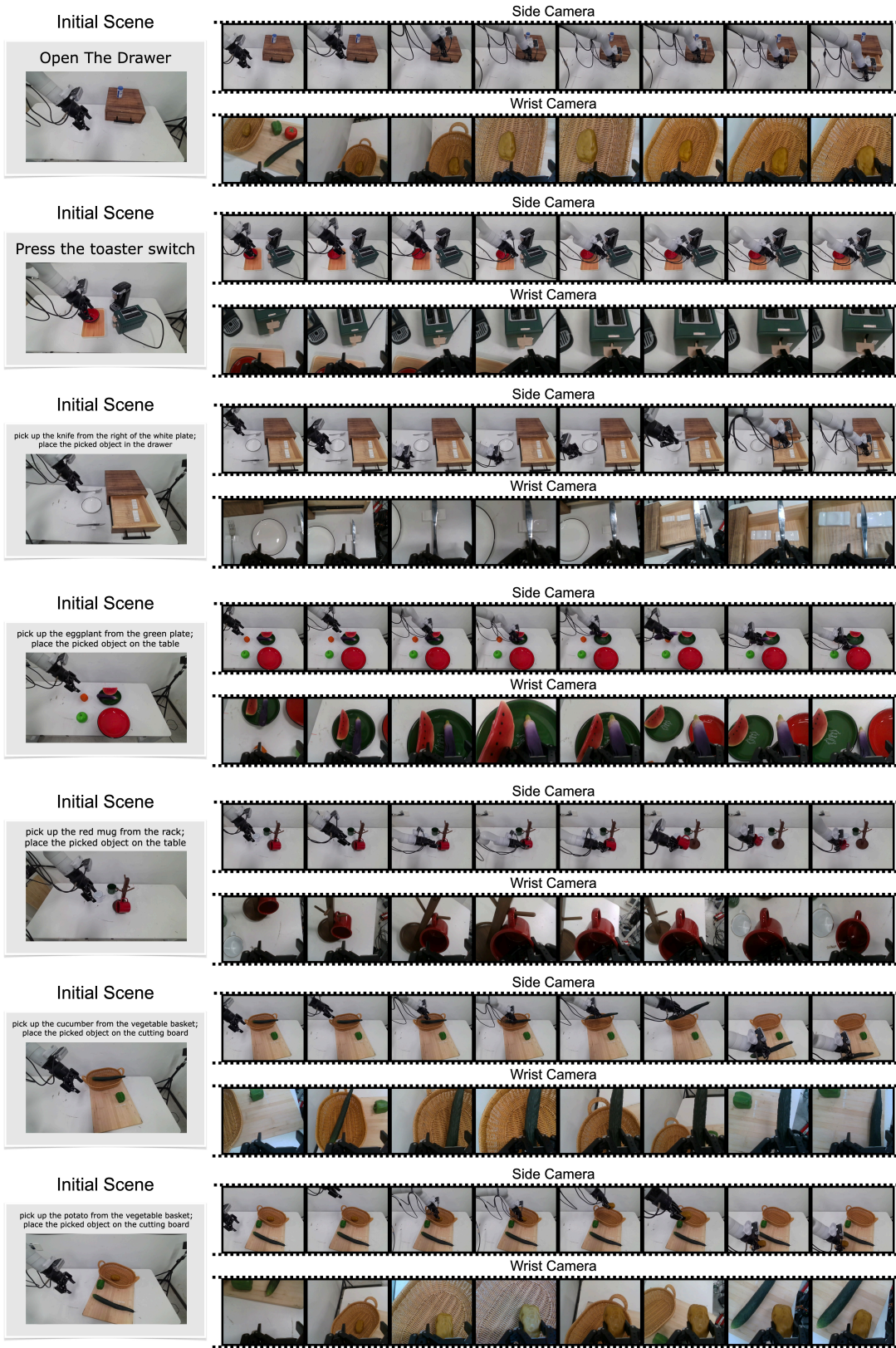


Supplementary Figure 1: Qualitative results for SimplerEnv tasks.

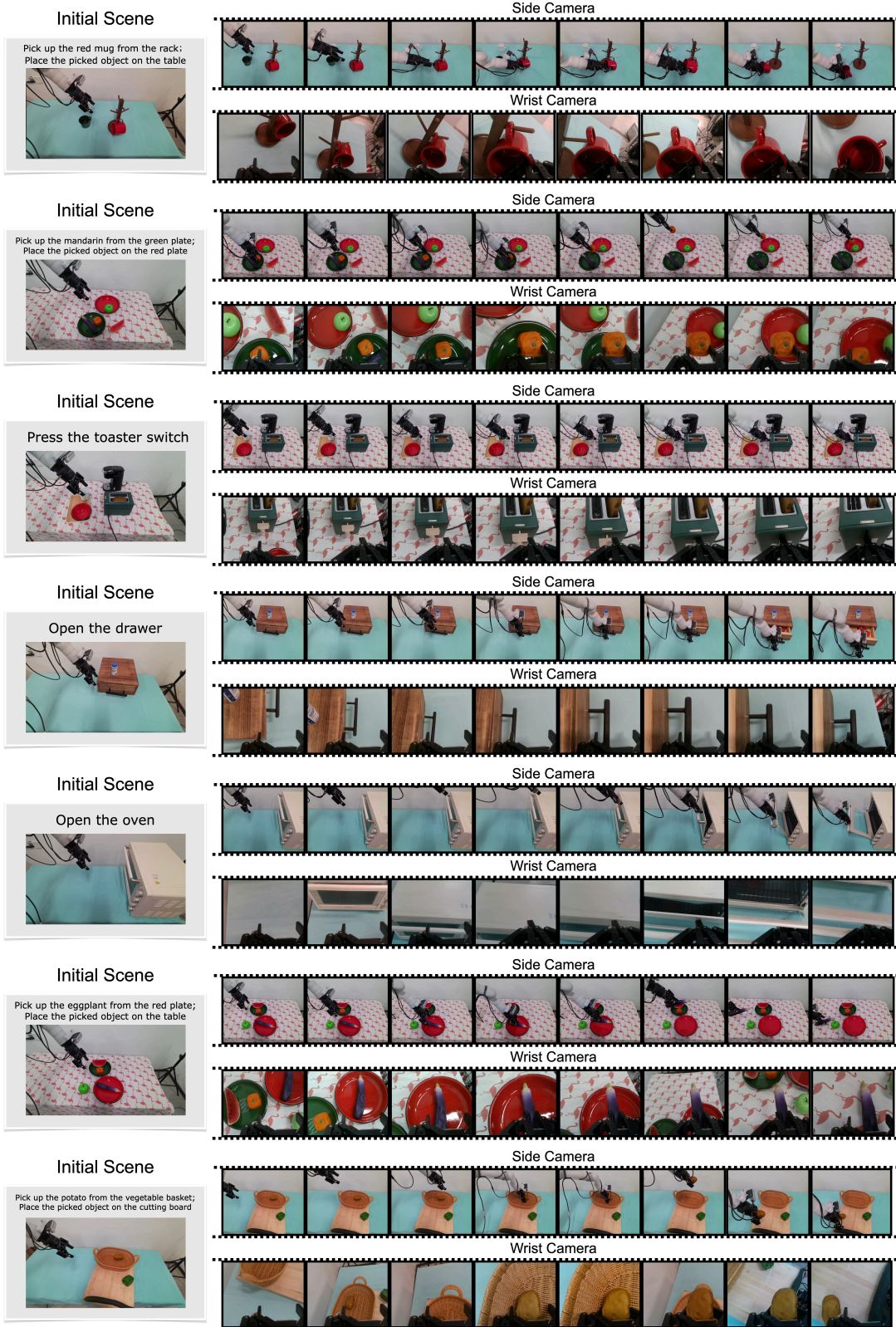
APPENDIX H ROLLOUT EXAMPLES IN REAL-WORLD EXPERIMENTS



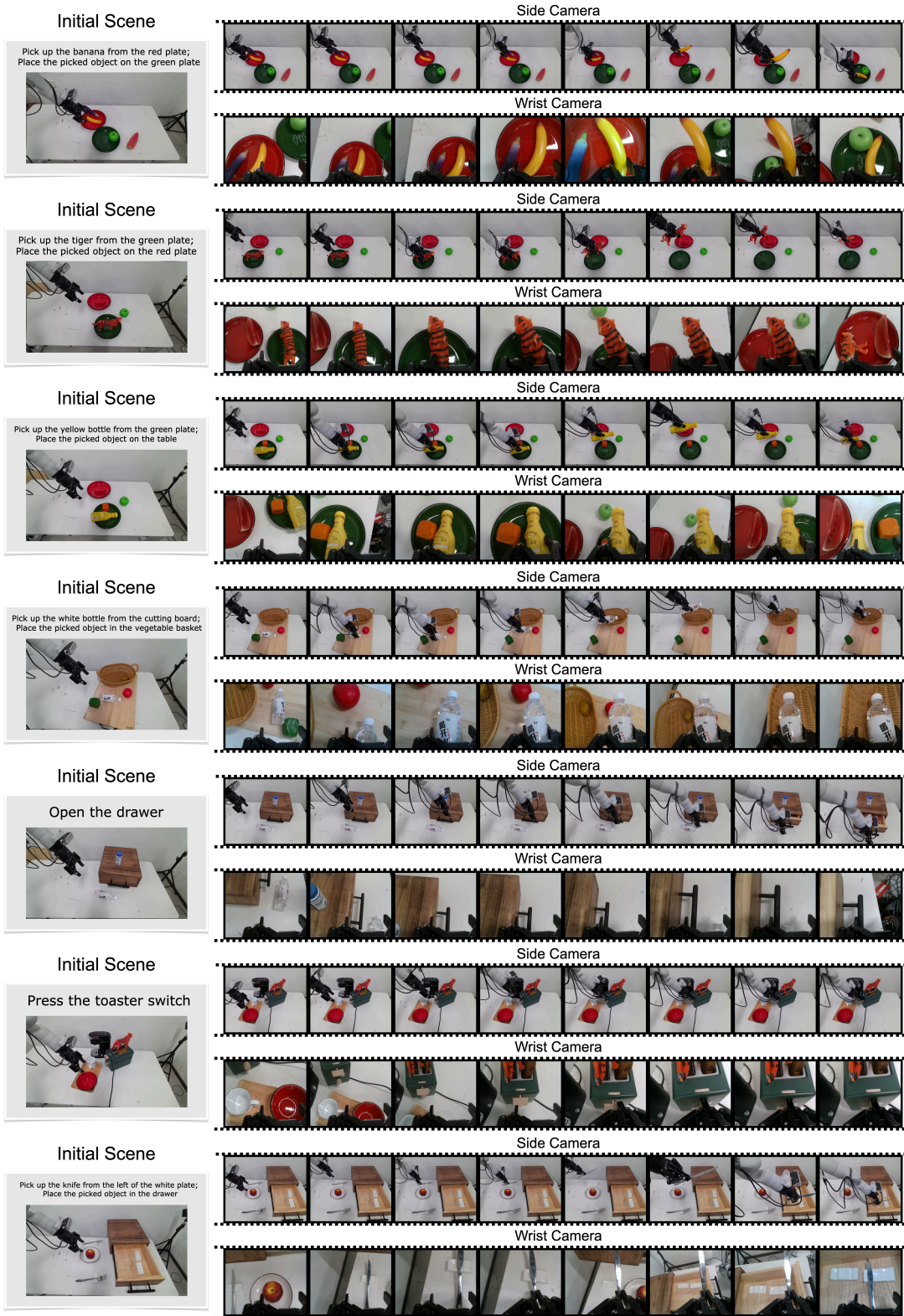
Supplementary Figure 2: This figure illustrates the experimental setup of some real-world tasks. The models are evaluated across 20 tasks, each with 5 rollouts, involving unseen distractors, unseen backgrounds, unseen target objects, and novel skill descriptions. Note that some tasks exclude the unseen target object setting due to the lack of suitable alternative unseen objects.



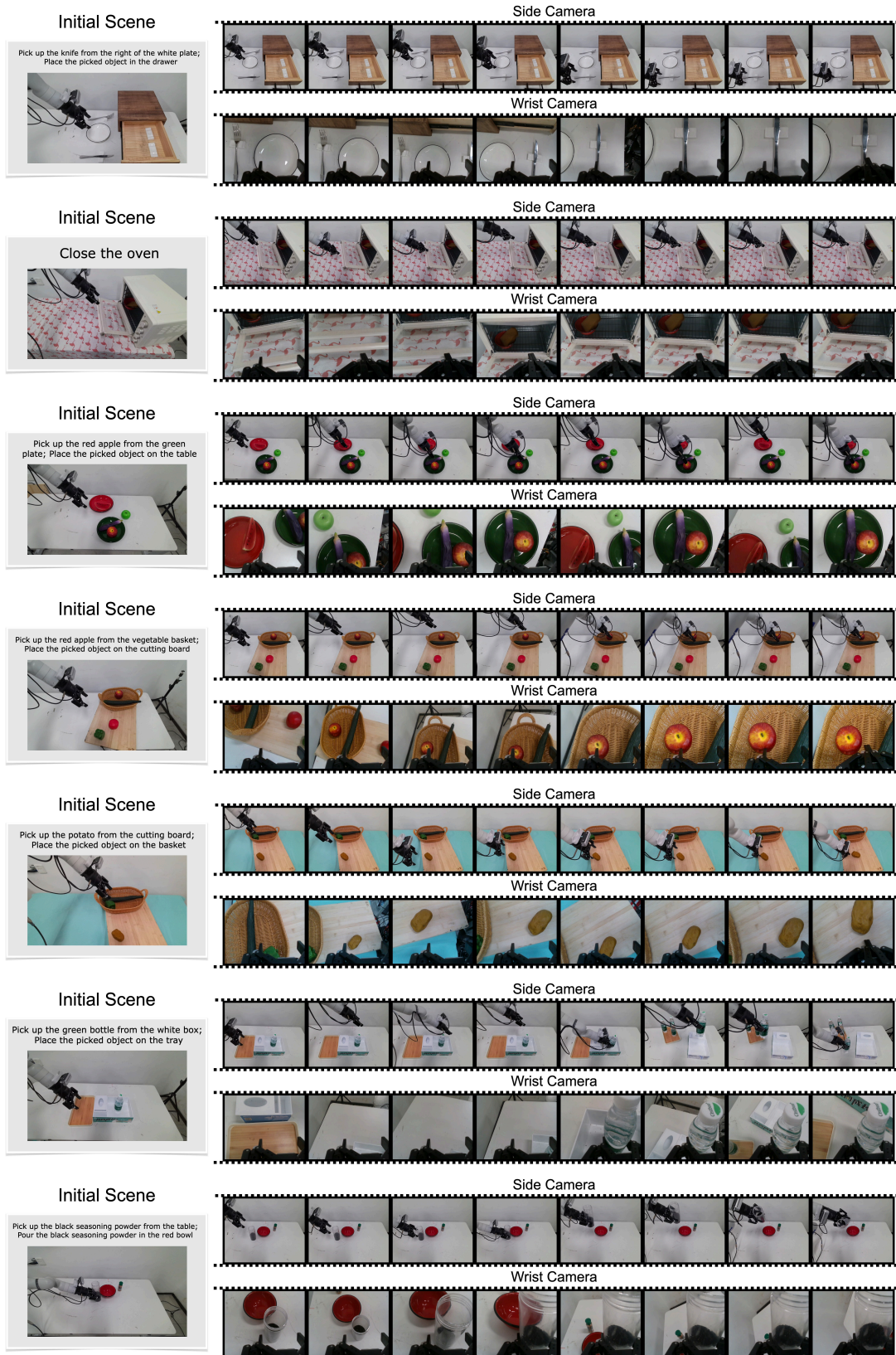
Supplementary Figure 3: Qualitative results for basic setting in real-world experiments.



Supplementary Figure 4: Qualitative results for unseen background.



Supplementary Figure 5: Qualitative results for unseen distractors and objects.



Supplementary Figure 6: Our model exhibits several typical failure cases. For instance, it might prematurely close the gripper, fail to accurately grasp the target object, exhibit repeated oscillations, or successfully pick up an object but cannot place it in the correct location.